6 December 2017

Dr. Nathalie Combourieu-Nebout, Editor Climate of the Past

Resubmission of Manuscript (Ref. No. cp-2017-104)

Dear Nathalie,

Thank so much for reconsidering our manuscript entitled "*Holocene climate aridification trend and human impact interrupted by millennial- and centennial-scale climate fluctuations from a new sedimentary record from Padul (Sierra Nevada, southern Iberian Peninsula)*", authored by María J. Ramos-Román, Gonzalo Jiménez-Moreno, Jon Camuera, Antonio García-Alix, R. Scott Anderson, Francisco J. Jiménez-Espejo, José S. Carrión, for publication in Climate of the Past. Here we are resubmitting the manuscript with minor revisions suggested by you of our previously submitted version of the manuscript (cp-2017-104).

We have gone in detail over all the very constructive suggestions that you made, which improved our manuscript. This revised manuscript complements point by point responses to your suggestions and comments.

We hope you find merit in this work and we look forward to hearing from you.

María J. Ramos-Román

Departamento de Estratigrafía y Paleontología

Universidad de Granada, Spain

Author's responses to the editor:

Firstly, we would like to thank the editor for reconsidering our manuscript for publication in Climate of the Past and accepting it after dealing with minor revision.

The editor suggestions and comments are displayed in black, and our answers are in blue. We indicate the lines in which we made the modifications according to the marked-up manuscript version (see below). In the case that we do not follow the editor suggestions we discussed the reasons.

Editor Decision: Publish subject to minor revisions (review by editor) (04 Dec 2017) by Nathalie Combourieu Nebout

Comments to the Author:

Dear authors,

I have read carefully all the comments of reviewers, your new version of the manuscript and the responses to reviewers you wrote.

You have amended your document and follow many requests from the three reviewers. Nevertheless some additional corrections are still needed before a complete acceptance of your manuscript.

My comments and requests are listed below:

1- It's a pity that you do not be able to present charcoal analyses to reinforce your interpretation. I agree with the reviewers. Would it be possible to add something on that even preliminary data with personal communication or indication to a paper in progress? That will help a lot.

Yes, we completely agree with you, however these data are not available yet. We are very sorry about that.

2- Generally I agree with the comments of all reviewers and especially with the comment 17 of Laura Sadori about your discussion. You have to demonstrate more in it and eventually to use additional data.

Laura Sadori's comment #17/ Line 401-403: you see… the two factors were probably overlapping. Who was the leading and starting one?
In my opinion (and in yours, I guess) it was climate, but this has to be demonstrated by independent data… that you, by the way, have.

We also think that the first and principal forcing controlling the aridification process was climate, detected by the forest depletion in response to the decrease in summer insolation. This is deduced as human impact in the area is not clear until the last 1550 cal yr BP. We believe that this is quite clear in this new version of the manuscript (see lines 38-41 in the abstract, discussion and conclusions). We also made a new figure, Figure 8, where we separated regional climate vs human impact proxies try to disentangling these two signals affecting the Padul environment.

3- I also completely agree with the reviewer asking you to describe first the basin (geology and so on) before describing the vegetation, the organization of the vegetation being strongly dependent from the geomorphology. In addition could you develop what the reviewer requested about the fact that the present day vegetation is to date completely modified by Human around the site?

In fact, I do not understand why you separate the Padul area description from the description of the Sierra Nevada. You describe first an altitudinal belt organization and after that another one typical to Padul, what is the links between the two??? Perhaps you may indicate the altitudinal belts corresponding to the Padul area and underlines the changes comparing to the theoretical association of the related belt and why it is modified. It would be easier to imagine a true representation of the landscape of the studied area. And please simplify the description of what is found in the Padul area as there are lot of plants that are not distinguishable through pollen.

This is a good point, thank you for your insight. After reading this paragraph again we agree with you that this is a bit confusing. In this new version we followed your suggestion and simplified this part of the text, joining those two previous sections (Sierra Nevada and Padul in one), simplifying this part considerably.
Please, see modifications (in section 2).

4- Would it be possible to have the indications of the AMS dates on the figure 3 and 4 to have an idea of the position of them? It would have been more pleasant to have first the pollen data versus depth to see the original data before having it in age or the have a reminder of the depth with the position of the datings on the diagram. Please .modify that.

Thank you for the suggestion. We added the AMS dating information to both figures and the depth scale to the lithology in the figure 4.

5- In the text, you do not indicate the changes in sedimentation rates, only the general fork, and they are indicated in the figure only. It remains important to note that the SR decrease strongly after 4 kyrs and re-increase in the ultimate upper part of the sequence. Have you an explanation of this SR changes? I have seen nothing in this part.

Yes, we agree that there was a lack of discussion about that subject and we added more information about this in the text. These changes are related with the evolution in the Padul environment. A decreasing trend in SR occurred after ca. 4 kyr, related with the decrease in organic material (TOC) and the increase in algae associated with higher water levels, this trend could be related with lower organic accumulation. The highest increase in SR occurred during the last century, which could be mainly associated due to the increase in clastic material as well as to a slight increase in TOC at that time.

Please, see modifications between lines (286-287; 540-543; 666).

6- As reviewer 2, I do not see any increase in Mediterranean forest nor in Quercus alone during PA2. In this zone I see a slight increase in Cichorioideae and a stabilization of Quercus in its general decreasing trend associated to a maximum of Ericaceae and Botryococcus. Please change that.

We tried to clarify that in the text indicating in lines 334-335 that the increase in Ericaceae and Cichoriodeae ocurred during zone PA2. A slight increase in deciduous *Quercus,* together with the increase in Ericaceae and *Botryococcus* also occurred during PA2b.

Please, see modification between lines (334-340).

7- You say that Botryococcus may be correlated to temperatures variations or I have not understand your discussion. I think it needs more explanations and I do not understand your response to reviewer 2 on that point.

Have you Cyanobacteria (AnaBaena for example) at the same time as Botryococcus to eventually reinforce the temperature effect? Generally Botryococcus increase indicates more increase in nutrient and partial increasing water level probably linked to more precipitation. For my part, in your record, I saw three phases: before 3kyr with low water level, between 3 kyrs and 1.5 kyr relatively high water level (increase in Botryococcus) and after 1.5 kyr general drying of the area and erosion? (decrease in Botryococcus and increase in Tilletia) with the area probably colonized by herbs and then by trees (probably planted by human??).

I think that you have to detail your demonstration to be more efficient concerning the links between your results and Bond events even if the climate probably may have a large influence (remember that coolings in Atlantic do not necessary mean coolings in Mediterranean but sometimes only aridity). Now I am not convinced by your correlations. For my part, I would prefer your remain moderate and discuss more about the increase and decrease water level correlated to different aridity events included into the general trend in aridity and perhaps linked to bond events. I agree with reviewer 2 and if you want to link all the curves you may also discuss the time lag that occurs between forest and Botryococcus and the fact that only few peaks are illustrated here. That's evident you have an increase of Mediterranean forest at the same time (a pause in the general aridity trend) but it occurs delayed from the botryococcus increase. You have to explain that.

I am sure that your data are not artefact but I suggest to moderate your interpretations concerning the figure 7 and 6.

Yes, *Botryococcus* is related here with freshwater lake environment and also with productivity, as there is a good correlation between *Botryococcus* and temperatures from the North Atlantic (see interpretation of proxies at the beginning of discussion, lines 418-422). Unfortunately, we did not record remains of cyanobacteria in our samples. We agree that we have different phases of water level (as we indicated in the degraded bar down in figure 5 and 8; and in section 4.4). We mostly interpreted the Padul environment as a shallow water lake (probably with higher water level and increase in productivity due humid and **warm** conditions) during the IRHP (maximum in *Botryococcus*); see lines 538-543) and after 1.5 ka BP a decrease in lake level, becoming an ephemeral lake, occurred when the *Botryococcus* and other algae began to decrease (see lines 590-593). This ephemeral lake phase was produced as consequence of a drying period (DA) after the IRHP, and was probably enhanced by the increase in human activity producing a higher soil erosion in the local environment connected with the increase

in *Tilletia* and other proxies relates with human land use in the environment since ca. 1.5 cal ka BP (see figure 8 and section 5.4).

In relation with your questions about the lag between forest and algae increase, it could be explained due to different responses between local and regional signal to climate variability, with regional signal (forest) mostly conditioned by precipitation and local (algae) also conditioned by temperature (productivity) and/or to different speed of the reaction of those two proxies to climate change (with algae logically responding faster). When maxima in both factors coincide, such as during the IRHP (wetter and warm phase), both proxies show their maximun values. We tried to clarify this in the text (lines 581-586), also moderating the language used for the correlations (579-580).

To avoid confusions and try to clarify our suggestions, we modified the figure 6 with a change in the *Botryococcus* curve interpretation, indicating that this as a productivity proxy instead of relative temperature.

8- In figure 6 the scale of the different curves do not express the true representation of the different proxies. Here they are artificially enlarged especially those of Botryococcus. Please draw the palynological curves with the same scale and draw the Bond curve in a reasonable scale not so much enlarged too.

Yes, the plots have been magnified in purpose in order to show the changes in the proxies in a very clear way. Even if the axes have been exaggerated, the magnitudes on the scales are correctly indicated and should not be a problem for the reader.

I think that my requests will not take so much time to be done and I am waiting after your response and new version of your manuscript.

Best regards,
Nathalie

Thank you so much

1 **Holocene climate aridification trend and human impact interrupted by millennial- and**
2 **centennial-scale climate fluctuations from a new sedimentary record from Padul (Sierra**
3 **Nevada, southern Iberian Peninsula)**

4 María J. Ramos-Román[1], Gonzalo Jiménez-Moreno[1], Jon Camuera[1], Antonio García-Alix[1],
5 R. Scott Anderson[2], Francisco J. Jiménez-Espejo[3], José S. Carrión[4]

6 [1] Departamento de Estratigrafía y Paleontología, Universidad de Granada, Spain
7 [2] School of Earth Sciences and Environmental Sustainability, Northern Arizona University,
8 USA.
9 [3] Department of Biogeochemistry, Japan Agency for Marine-Earth Science and Technology
10 (JAMSTEC), Japan.
11 [4] Departamento de Biología Vegetal, Facultad de Biología, Universidad de Murcia, Murcia,
12 Spain.

13 *Correspondence to:* María J. Ramos-Román (mjrr@ugr.es)

14 **Abstract.** Holocene centennial-scale paleoenvironmental variability has been described in a
15 multiproxy analysis (i.e. lithology, geochemistry, macrofossil and microfossil analyses) of a
16 paleoecological record from the Padul basin in Sierra Nevada, southern Iberian Peninsula.
17 This sequence covers a relevant time interval hitherto unreported in the studies of the Padul
18 sedimentary sequence. The ~4700 yr-long record has preserved proxies of climate variability,
19 with vegetation, lake levels and sedimentological change during the Holocene in one of the
20 most unique and southernmost wetland from Europe. The progressive Middle and Late
21 Holocene trend toward arid conditions identified by numerous authors in the western
22 Mediterranean region, mostly related to a decrease in summer insolation, is also documented
23 in this record, being here also superimposed by centennial-scale variability in humidity. In
24 turn, this record shows centennial-scale climate oscillations in temperature that correlate with
25 well-known climatic events during the Late Holocene in the western Mediterranean region,
26 synchronous with variability in solar and atmospheric dynamics. The multiproxy Padul
27 record first shows a transition from a relatively humid Middle Holocene in the western
28 Mediterranean region to more aridity from ~4700 to ~2800 cal yr BP. A relatively warm and
29 humid period occurred between ~2600 to ~1600 cal yr BP, coinciding with persistent
30 negative NAO conditions and the historic Iberian-Roman Humid Period. Enhanced arid
31 conditions, co-occurring with overall positive NAO conditions and increasing solar activity,
32 are observed between ~1550 to ~ 450 cal yr BP (~400 to ~1400 CE) and colder and warmer
33 conditions happened during the Dark Ages and Medieval Climate Anomaly, respectively.
34 Slightly wetter conditions took place during the end of the MCA and the first part of the
35 Little Ice Age, which could be related to a change towards negative NAO conditions and
36 minima in solar activity. Time series analysis performed from local (*Botryococcus* and TOC)
37 and regional (Mediterranean forest) signals helped us determining the relationship between
38 southern Iberian climate evolution, atmospheric, oceanic dynamics and solar activity. Our
39 multiproxy record shows little evidence of human impact in the area until ~1550 cal yr BP,
40 when evidence of agriculture and livestock grazing occurs. Therefore climate is the main
41 forcing mechanism controlling environmental change in the area until relatively recently.

43 **Keywords:** Holocene, Padul**,** peat bog, North Atlantic Oscillation, atmospheric dynamics,
44 southern Iberian Peninsula, Sierra Nevada, western Mediterranean.

Deleted: peat bogs

1   Introduction

The Mediterranean area is situated in a sensitive region between temperate and subtropical climates making it an important place to study the connections between atmospheric and oceanic dynamics and environmental change. Climate in the western Mediterranean and the southern Iberian Peninsula is influenced by several atmospheric and oceanic dynamics (Alpert et al., 2006), including the North Atlantic Oscillation (NAO) one of the principal atmospheric phenomenon controlling climate in the area (Hurrell, 1995; Moreno et al., 2005). Recent NAO reconstructions in the western Mediterranean relate negative and positive NAO conditions with an increase and decrease, respectively, in winter (effective) precipitation (Olsen et al., 2012; Trouet et al., 2009). Numerous paleoenvironmental studies in the western Mediterranean have detected a link at millennial- and centennial-scales between the oscillations of paleoclimate proxies from sedimentary records with solar variability and atmospheric (i.e., NAO) and/or ocean dynamics during the Holocene (Fletcher et al., 2013; Moreno et al., 2012; Rodrigo-Gámiz et al., 2014). Very few montane and low altitude lake records in southern Iberia document centennial-scale climate change [see, for example Zoñar Lake (Martín-Puertas et al., 2008)], with most terrestrial records in the western Mediterranean region evidencing only millennial-scale cyclical changes. Therefore, higher-resolution decadal-scale analyses are necessary to analyze the link between solar activity, atmospheric and oceanographic systems with terrestrial environment in this area at shorter (i.e., centennial) time scales.

Sediments from lakes, peat bogs and marine records from the western Mediterranean have documented an aridification trend during the Late Holocene (Carrión et al., 2010; Gil-Romera et al., 2010; Jalut et al., 2009). This trend, however, was superimposed by shorter-term climate variability, as shown by several recent studies from the region (Carrión, 2002; Fletcher et al., 2013; Jiménez-Moreno et al., 2013; Martín-Puertas et al., 2008; Ramos-Román et al., 2016). This relationship between climate variability, culture evolution and human impact during the Late Holocene has also been the subject of recent paleoenvironmental studies (Carrión et al., 2007; Lillios et al., 2016; López-Sáez et al., 2014; Magny, 2004). However, it is still unclear whether climate or human activities have been the main forcing driving environmental change (i.e., deforestation) in this area during this time.

Within the western Mediterranean, Sierra Nevada is the highest and southernmost mountain range in the Iberian Peninsula and thus presents a critical area for paleoenvironmental studies. Most high-resolution studies there have come from high elevation sites. The well-known Padul wetland site is located at the western foot of the Sierra Nevada (Fig. 1) and bears one of the longest continental records in southern Europe, with a sedimentary sequence of ~100 m thick that could represent the last 1 Ma (Ortiz et al., 2004). Several research studies, including radiocarbon dating, geochemistry and pollen analyses, have been carried out on previous cores from Padul, and have documented glacial/interglacial cycles during the Pleistocene and up until the Middle Holocene. However, the Late Holocene section of the Padul sedimentary sequence has never been effectively retrieved and studied (Florschütz et al., 1971; Ortiz et al., 2004; Pons and Reille, 1988). This was due to the location of these previous corings within a current peat mine operation, where the upper (and non- productive) part of the sedimentary sequence was missing.

Here we present a new record from the Padul basin: Padul-15-05, a 42.64 m-long sediment core that, for the first time, contains a continuous record of the Late Holocene (Fig. 2). A high-resolution multi-proxy analysis of the upper 1.15 m, the past ~4700 cal yr BP, has

| Deleted: peat bog |

| Deleted: peat bog |

97 allowed us to determine a complete paleoenvironmental and paleoclimatic record at
98 centennial- and millennial-scales. To accomplish that, we reconstructed changes in the Padul
99 vegetation, sedimentation, climate and human impact during the Holocene throughout the
100 interpretation of the lithology, palynology and geochemistry.

102 Specifically, the main objective of this paper is to determine environmental variability and
103 climate evolution in the southern Iberian Peninsula and the western Mediterranean region and
104 their linkages to northern hemisphere climate and solar variability during the latter Holocene.
105 In order to do this, we compared our results with other paleoclimate records from the region
106 and solar activity from the northern hemisphere for the past ~4700 cal yr BP (Bond et al.,
107 2001; Laskar et al., 2004; Sicre et al., 2016; Steinhilber et al., 2009).

2 Regional setting: Padul climate and vegetation

109 Padul is located at the foothill of Sierra Nevada, which is a W-E aligned mountain range
110 located in Andalucía (southern Spain; Fig. 1). Climate in this area is Mediterranean, with cool
111 and humid winters and hot/warm summer drought. Sierra Nevada is strongly influenced by
112 thermal and precipitation variations due to the altitudinal gradient (from ca. 700 to more than
113 3400 m), which control plant taxa distribution in different bioclimatic vegetation belts due to
114 the variability in thermotypes and ombrotypes (Valle Tendero, 2004). According to the
115 climatophilous series classification, Sierra Nevada is divided in four different vegetation belts
116 (Fig. 1). The crioromediterranean vegetation belt, occurring above ~2800 m, is characterized
117 by tundra vegetation and principally composed by species of Poaceae, Asteraceae,
118 Brassicaceae, Gentianaceae, Scrophulariaceae and Plantaginaceae between other herbs, with
119 a number of endemic plants (e.g. *Erigeron frigidus, Saxifraga nevadensis, Viola crassiuscula,*
120 *Plantago nivalis*). The oromediterranean belt, between ~ 1900 to ~2800 m, is principally
121 made up of *Pinus sylvestris*, *P. nigra* and *Juniperus* spp. and other shrubs such as species of
122 Fabaceae, Cistaceae and Brassicaceae. The supramediterranean belt, from ~ 1400 to 1900 m
123 of elevation, bears principally *Quercus pyrenaica*, *Q. faginea* and *Q. rotundifolia* and *Acer*
124 *opalus* ssp. *granatense* with other trees and shrubs, including members of the Fabaceae,
125 Thymelaeaceae, Cistaceae and *Artemisia* sp. being the most important. The
126 mesomediterranean vegetation belt occurs between ~600 and 1400 m of elevation and is
127 principally characterized by *Quercus rotundifolia*, some shrubs, herbs and plants as *Juniperus*
128 sp., and some species of Fabaceae, Cistaceae and Liliaceae with others (El Aallali et al.,
129 1998; Valle, 2003). The human impact over this area, especially important during the last
130 millennium, affected the natural vegetation distribution through fire, deforestation,
131 cultivation (i.e., *Olea*) and subsequent reforestation (mostly *Pinus*) (Anderson et al., 2011).
132 The Padul basin is situated in the mesomediterranean vegetation belt at approximately 725 m
133 elevation in the southeastern part of the Granada Basin. In this area and besides the
134 characteristic vegetation at this elevation, nitrophilous communities occur in soils disrupted
135 by livestock, pathways or open forest, normally related with anthropization (Valle, 2003).
136 This is one of the most seismically active areas in the southern Iberian Peninsula with
137 numerous faults in NW-SE direction, with the Padul fault being one of these active normal
138 faults (Alfaro et al., 2001). It is a small extensional basin approximately 12 km long and
139 covering an area of approximately 45 km^2, which is bounded by the Padul normal fault. The
140 sedimentary in-filling of the basin consists of Neogene and Quaternary deposits; Upper
141 Miocene conglomerates, calcarenites and marls, and Pliocene and Quaternary alluvial
142 sediments, lacustrine and peat bog deposits (Sanz de Galdeano et al., 1998; Delgado et al.,
143 2002; Domingo et al., 1983).

184 The Padul wetland is endorheic, with a surface of approximately 4 km^2 placed in the Padul
185 basin that contains a sedimentary sequence characterized mostly by peat accumulation. The
186 basin fill is asymmetric, with thicker sedimentary and peat infill to the northeast (~100 m
187 thick; Domingo-García et al., 1983; Florschütz et al., 1971; Nestares and Torres, 1997) and
188 progressively becoming thinner to the southwest (Alfaro et al., 2001). The main source area
189 of allochthonous sediments in the bog is the Sierra Nevada, which is characterized at higher
190 elevations by Paleozoic siliceous metamorphic rocks (mostly mica-schists and quartzites)
191 from the Nevado-Filabride complex and, at lower elevations and acting as bedrock, by
192 Triassic dolomites, limestones and phyllites from the Alpujárride Complex (Sanz de
193 Galdeano et al. 1998). Geochemistry in the Padul sediments is influenced by detritic
194 materials also primarily from from the the Sierra Nevada (Ortiz et al., 2004). Groundwater
195 inputs into the Padul basin come from the Triassic carbonates aquifers (N and S edge to the
196 basin), the out flow of the Granada Basin (W edge to the basin) and the conglomerate aquifer
197 to the east edge (Castillo Martín et al., 1984; Ortiz et al., 2004). The main water output is by
198 evaporation and evapotranspiration, water wells and by canals ("madres") that drain the water
199 to the Dúrcal river to the southeast (Castillo Martín et al., 1984). Climate in the Padul area is
200 characterized by a mean annual temperature of 14.4 ºC and a mean annual precipitation of
201 445 mm (http://www.aemet.es/).
202 The Padul-15-05 drilling site was located ~50 m south of the present-day Padul lake shore
203 area. This basin area is presently subjected to seasonal water level fluctuations and is
204 principally dominated by *Phragmites australis* (Poaceae). The lake environment is dominated
205 by aquatic and wetland communities with *Chara vulgaris*, *Myriophyllum spicatum*,
206 *Potamogeton pectinatus*, *Potamogetum coloratus*, *Phragmites australis*, *Typha*
207 *dominguensis*, *Apium nodiflorum*, *Juncus subnodulosus*, *J. bufonius*, *Carex hispida and*
208 *Ranunculus muricatus,* among others (Pérez Raya and López Nieto, 1991). Some sparse
209 riparian trees occur in the northern lake shore, such as *Populus alba*, *Populus nigra*, *Salix* sp.,
210 *Ulmus minor* and *Tamarix*. At present *Phragmites australis* is the most abundant plant
211 bordering the lake. Surrounding this area are cultivated crops with cereals, such as *Triticum*
212 spp., as well as *Prunus dulcis* and *Olea europea*.

3 Material and methods

215 Two sediment cores, Padul-13-01 (37º00'40''N; 3º36'13''W) and Padul-15-05
216 (37º00'39.77''N; 3º36'14.06''W) with a length of 58.7 cm and 42.64 m, respectively, were
217 collected between 2013 and 2015 from the wetland (Fig. 1). The cores were taken using a
218 Rolatec RL-48-L drilling machine equipped with a hydraulic piston corer from the Scientific
219 Instrumentation Centre of the University of Granada (UGR). The sediment cores were
220 wrapped in film, put in core boxes, transported to UGR and stored in a dark cool room at 4ºC.

3.1 Age-depth model (AMS radiocarbon dating)

222 The core chronology was constrained using fourteen AMS radiocarbon dates from plant
223 remains and organic bulk samples taken from the cores (Table 1). In addition, one sample
224 with gastropods was also submitted for AMS radiocarbon analysis, although it was rejected
225 due to important reservoir effect, that provided a very old date. Thirteen of these samples
226 came from Padul-15-05 with one from the nearby Padul-13-01 (Table 1). We were able to
227 use this date from Padul-13-01 core as there is a very significant correlation between the
228 upper part of Padul-15-05 and Padul-13-01 cores, shown by identical lithological and
229 geochemical changes (Supplementary information 1; Figure S1). The age model for the upper

232 ~3 m minus the upper 21 cm from the surface was built using the R-code package 'Clam 2.2'
233 (Blaauw, 2010) employing the calibration curve IntCal 13 (Reimer et al., 2013), a 95 % of
234 confidence range, a smooth spline (type 4) with a 0.20 smoothing value and 1000 iterations
235 (Fig. 2). The chronology of the uppermost 21 cm of the record was built using a linear
236 interpolation between the last radiocarbon date and the top of the record (Present; 2015 CE).
237 Even though the length of the Padul-15-05 core is ~43 m, the studied interval in the work
238 presented here is the uppermost 115 cm of the record that are constrained by seven AMS
239 radiocarbon dates (Fig. 2).

3.2 Lithology, MS, XRF and TOC

241 Padul-15-05 core was split longitudinally and was described in the laboratory with respect to
242 lithology and color (Fig. 3). Magnetic susceptibility (MS) was measured with a Bartington
243 MS3 operating with a MS2E sensor. MS measurements (in SI units) were obtained directly
244 from the core surface every 0.5 cm (Fig. 3).

246 Elemental geochemical composition was measured in an X-Ray fluorescence (XRF)
247 Avaatech core scanner® at the University of Barcelona (Spain). A total of thirty-three
248 chemical elements were measured in the XRF core scanner at 10 mm of spatial resolution,
249 using 10 s count time, 10 kV X-ray voltage and a X-ray current of 650 μA for lighter
250 elements and 35 s count time, 30 kV X-ray voltage, X-ray current of 1700 μA for heavier
251 elements. Thirty-three chemical elements were measured but only the most representative
252 with a major number of counts were considered (Si, K, Ca, Ti, Fe, Zr, Br and Sr). Results for
253 each element are expressed as intensities in counts per second (cps) and normalized (norm.)
254 for the total sum in cps in every measure (Fig. 3).
255 Total organic carbon (TOC) was analyzed every 2 or 3 cm throughout the core. Samples were
256 previously decalcified with 1:1 HCl in order to eliminate the carbonate fraction. The
257 percentage of organic Carbon (OC %) was measured in an Elemental Analyzer Thermo
258 Scientific Flash 2000 model from the Scientific Instrumentation Centre of the UGR (Spain).
259 Percentage of TOC per gram of sediment was calculated from the percentage of organic
260 carbon (OC %) yielded by the elemental analyzer, and recalculated by the weight of the
261 sample prior to decalcification (Fig. 3).

3.3 Pollen and NPP

263 Samples for pollen analysis (1-3 cm^3) were taken every 1 cm throughout the core, with a total
264 of 103 samples analyzes. Pollen extraction methods followed a modified Faegri and Iversen
265 (1989) methodology. Processing included the addition of *Lycopodium* spores for calculation
266 of pollen concentration. Sediment was treated with NaOH, HCl, HF and the residue was
267 sieved at 250 μm previous to an acetolysis solution. Counting was performed using a
268 transmitted light microscope at 400 magnifications to an average pollen count of ca. 260
269 terrestrial pollen grains. Fossil pollen was identified using published keys (Beug, 2004) and
270 modern reference collections at University of Granada (Spain). Pollen counts were
271 transformed to pollen percentages based on the terrestrial pollen sum, excluding aquatics.
272 The palynological zonation was executed by cluster analysis using twelve primary pollen
273 taxa- *Olea*, *Pinus*, deciduous *Quercus*, evergreen *Quercus*, *Pistacia*, Ericaceae, *Artemisia*,
274 Asteroideae, Cichorioideae, Amaranthaceae and Poaceae (Grimm, 1987) (Fig. 4). Non-pollen
275 palynomorphs (NPP) include fungal and algal spores, and thecamoebians (testate amoebae).
276 The NPP percentages were calculated and represented with respect to the terrestrial pollen
277 sum (Fig. 4). Furthermore, some pollen taxa were grouped, according to present-day

278 ecological bases, into Mediterranean forest and xerophytes (Fig. 4). The Mediterranean forest
279 taxa is composed of *Quercus* total, *Olea*, *Phillyrea* and *Pistacia*. The xerophyte group
280 includes *Artemisia*, *Ephedra*, and Amaranthaceae.

281 **4 Results**

282 **4.1 Chronology and sedimentation rates**

283 The age-model of the upper 115 cm of Padul-15-05 core (Fig. 2) shows an average
284 sedimentation rate (SAR) of 0.058 cm/yr over last ~4700 cal yr BP, being the age constrained
285 by seven AMS ^{14}C dates (Table 1). However, SARs of individual core segments vary from
286 0.01 to 0.16 cm/yr (Fig. 2), showing the lowest values between ~51 and 40 cm (from ~2600
287 to 1350 cal yr BP) and the highest values during the last ~20 cm (last century).

288 **4.2 Lithology, MS, XRF and TOC**

289 The stratigraphy of the upper ~115 cm of the Padul-15-05 sediment core was deduced
290 primarily by visual inspection. However, our visual inspections were support by comparison
291 with the element geochemical composition (XRF), the MS of the split cores, and TOC (Fig.
292 3) to determine shifts in sediment facies. The lithology for this sedimentary sequence consists
293 in clays with variable carbonates, siliciclastics and organic content (Fig. 3). We also used a
294 Linear r (Pearson) correlation to calculated relationship for the XRF data. The correlation for
295 the inorganic geochemical elements determined two different groups of elements that covary
296 (Table 2): Group 1) Si, K, Ti, Fe and Zr with a high positive correlation between them;
297 Group 2) Ca, Br and Sr have negative correlation with Group 1. Based on this, the sequence
298 is subdivided in two principal sedimentary units. The lower ~87 cm of the record is
299 designated to Unit 1, characterized principally by relatively low values of MS and higher
300 values of Ca. The upper ~28 cm of the sequence is designated to Unit 2, in which the
301 mineralogical composition is lower in Ca with higher values of MS in correlation with mostly
302 siliciclastics elements (Si, K, Ti, Fe and Zr).
303
304 Within these two units, four different facies can be identified by visual inspection and by the
305 elemental geochemical composition and TOC of the sediments. *Facies* 1 (115-110 cm depth,
306 ~4700 to 4650 cal yr BP; and 89-80 cm depth ~4300 to 4000 cal yr BP) are characterized by
307 dark brown organic clays that bear charophytes and macroscopic plant remains. They also
308 have depicted relative higher values of TOC values (Fig. 3). *Facies* 2 (110-89 cm depth
309 ~4650 to 4300 cal yr BP; and 80-42 cm depth, ~4000 to 1600 cal yr BP) is compose of brown
310 clays, with the occurrence of gastropods and charophytes. This facies is also characterized by
311 lower TOC values. *Facies* 3 (42-28 cm depth, ~1600 to 400 cal yr BP) is characterized by
312 grayish brown clays with the occurrence of gastropods, and lower values of TOC, and an
313 increasing trend in MS and in siliciclastic elements. *Facies* 4 (28-0 cm, ~400 cal yr BP to
314 Present) is made up of light grayish brown clays and features a strong increase in siliciclastic
315 linked to a strong increase in MS.

316 **4.3 Pollen and NPP**

317 Several terrestrial and aquatic pollen taxa were identified but only the most representative
318 taxa are here plotted in the summary pollen diagram (Fig. 4). Selected NPP percentages are
319 also displayed in Figure 4. Four pollen zones (PA) were visually identified with the help of a
320 cluster analysis using the program CONISS (Grimm, 1987). Pollen concentration was higher
321 during Unit 1 with a decreasing trend in the transition to Unit 2 and a later increase during the

322   pollen subzone PA-4b (Fig. 4). Pollen zones are described below:

4.3.1 Zone PA-1 [~4720 to 3400 cal yr BP/ ~2800 to 1450 BCE (115-65 cm)]

324   Zone 1 is characterized by the abundance of Mediterranean forest species reaching up to ca.
325   70 %. Another important taxon in this zone is *Pinus,* with average values around 18 %. Herbs
326   are largely represented by Poaceae, averaging around 10 %, and reaching up to ca. 25 %.
327   This pollen zone is subdivided into PA-1a, PA-1b and PA-1c (Fig. 4). The principal
328   characteristic that differentiating PA-1a from PA-1b (boundary at ~4650 cal yr BP/~2700
329   BCE) is the decrease in Poaceae, the increase in *Pinus*, and the appearance of cf. *Vitis*. The
330   subsequent decrease in Mediterranean forest pollen to average values around 40 %, the
331   increase in *Pinus* to average ~25 % and a progressive increase in Ericaceae to ~6 to 11 %,
332   distinguishes subzones PA-1b and PA-1c (boundary at ca. 3950 cal yr BP).

4.3.2. Zone PA-2 [~3400 to 1550 cal yr BP/~1450 BCE to 400 CE (65-41 cm)]

334   The main features of this zone are the increase in Ericaceae up to ~16 %, some herbs such as
335   Cichorioideae, became more abundant reaching average percentages of ~7 %. This pollen
336   zone can be subdivided in subzones PA-2a and PA-2b with a boundary at ~2850 cal yr BP
337   (~900 BCE). The principal characteristics that differentiate these subzones is marked by the
338   increasing trend in Ericaceae and deciduous *Quercus* reaching maximum values of ~30 %
339   and ~20 %, respectively. In addition, the increase in *Botryococcus,* which averages from ~4
340   to 9 %. Also notable is the expansion of *Mougeotia* and *Zygnema* types.

4.3.3 Zone PA-3 [~1550 to 400 cal yr BP/~400 CE to 1550 CE (41-29 cm)]

342   This zone is distinguished by the continuing decline of Mediterranean forest elements.
343   Cichorioideae reached average values of about 40 %, and is paralleled by the decrease in
344   Ericaceae. A decline in *Botryococcus* and other algal remains is also observed in this zone,
345   although there is an increase in total Thecamoebians from average of <1 % to 10 %. This
346   pollen zone is subdivided in subzones PA-3a and PA-3b at ~1000 cal yr BP (~950 CE). The
347   main features that differentiate these subzones are the increase in *Olea* from subzone PA-3a
348   to PA-3b from average values of ~1 to 5 %. The increasing trend in Poaceae is also a feature
349   in this subzone, as well as the slight increase in Asteroideae at the top. Significant changes
350   are documented in NPP percentages in this subzone with the increase of some fungal remain
351   such as *Tilletia* and *Glomus* type. Furthermore, a decrease in *Botrycoccus* and the near
352   disappearance of other algal remains such as *Mougetia* occurred.

4.3.4 Zone PA-4 [~last 400 cal yr BP/ ~ 1550 CE to Present (29-0 cm)]

354   The main feature in this zone is the significant increase in *Pinus,* reaching maximum values
355   of ~32 %, an increase in Poaceae to ~40 %) and the decrease in Cichorioideae (~44 to 16 %).
356   Other important changes are the nearly total disappearance of some shrubs such as *Pistacia*
357   and a decreasing trend in Ericaceae, as well as a further decline in Mediterranean forest
358   pollen. An increase in wetland pollen taxa, mostly *Typha*, also occurred. A significant
359   increase in xerophytes, mostly Amaranthaceae to ~14 % is also observed in this period. Other
360   herbs such as *Plantago*, Polygonaceae and Convolvulaceae show moderate increases. PA-4 is
361   subdivided into subzones PA-4a and PA-4b (Fig. 4). The top of the record (PA-4b), which
362   corresponds with the last ~120 yr, is differentiated from subzone PA-4a (from ~400 – 120 cal
363   yr BP) by a decline in some herbs such as Cichorioideae. However, an increase in other herbs
364   such as Amaranthaceae and Poaceae occurred. The increase in *Plantago* is also significant

during this period. PA-4b also has a noteworthy increase in *Pinus* (from ~14 to 27 %) and a slight increase in *Olea* and evergreen *Quercus* are also characteristic of this subzone. With respect to NPPs, thecamoebians such as *Arcella* type and in the largely coprophilous sordariaceous (Sordariales) spores also increase. This zone also documents the decrease in fresh-water algal spores, in *Botryococcus* concomitant with *Mougeotia and Zygnema type*.

4.4 Estimated lake level reconstruction

Different local proxies from the Padul-15-05 record [Si, Ca, TOC, MS, hygrophytes (Cyperaceae and *Typha*), Poaceae and algae (including *Botryoccocus*, *Zygnema* types and *Mougeotia*) groups] have been depicted in order to understand the relationship between lithological, geochemical, and palynological variability and the water lake level oscillations. Sediments with higher values of TOC (more algae and hygrophytes) and rich in Ca (related with the occurrence of shells and charophytes remains) most likely characterized a shallow water environment (Unit 1). The continuous decline in *Botryococcus*, the disappearance of charophytes and the progressively increase in detritics (increase in MS and Si values) could be associated with shallower and even ephemeral lake environment (transition from Unit 1 to Unit 2; ~41 to 28 cm). The absence of aquatic remains, almost disappearance of *Botryococcus* and decreasing Ca and a lower TOC and/or a higher input of clastic material (higher MS and Si values) into the lake, could be related with lake level lowering, and even emerged conditions (increase in Poaceae; Unit 2) (Fig. 5).

4.5 Spectral analysis

Spectral analysis was performed on selected pollen and NPP time series (Mediterranean forest and *Botryococcus)*, as well as TOC in order to identify millennial- and centennial-scale periodicities. The mean sampling resolution for pollen and NPP is ~50 yr and for geochemical data is ~80 yr. Statistically significant cycles, above the 90, 95 and 99 % of confident levels, were found around 800, 680, 300, 240, 200, 170 (Fig. 7).

5 Discussion

Numerous proxies have been used in this study to interpret the paleoenvironmental and hydrodynamic changes recorded in the Padul sedimentary record during the last 4700 cal yr BP. Palynological analysis (pollen and NPP) is commonly used as a proxy for vegetation and climate change, and lake level variations, as well as human impact and land uses (e.g. Faegri and Iversen, 1990; van Geel et al., 1983). Disentangling natural vs. anthropogenic effects on the environment in the last millennials is sometimes challenging but can be persuaded using a multi-proxy approach (Roberts et al., 2011; Sadori et al., 2011). In this study, we used the variations between Mediterranean forest taxa, xerophytes and algal communities for paleoclimatic variability and the occurrence of nitrophilous and ruderal plant communities and some NPPs for identifying human influence in the study area. Variations in arboreal pollen (AP, including Mediterranean tree species) have previously been used in previous Sierra Nevada records as a proxy for humidity changes (Jiménez-Moreno and Anderson, 2012; Ramos-Román et al., 2016). The increase or decrease in Mediterranean forest species has been used as a proxy for climate change in other studies in the western Mediterranean region, with greater forest development generally meaning higher humidity (Fletcher et al., 2013; Fletcher and Sánchez-Goñi, 2008). On the other hand, increases in xerophyte pollen taxa (i.e., *Artemisia*, *Ephedra*, Amaranthaceae) have been used as an indication of aridity in this area (Anderson et al., 2011; Carrión et al., 2007).

The chlorophyceae alga *Botryococcus* sp. has been used as an indicator of freshwater environments, in relatively productive fens, temporary pools, ponds or lakes (Guy-Ohlson, 1992). The high visual and statistical correlation between *Botryococcus* from Padul-15-05 and North Atlantic temperature estimations [Bond et al., 2001; r = -0.63; $p < 0.0001$; between ca. 4700 to 1500 cal yr BP and r=-0.48; $p < 0.0001$ between 4700 and -65 cal yr BP (the decreasing and very low *Botryococcus* occurrence in the last 1500 cal yr BP makes this correlation moderate)] seems to show that in this case *Botryococcus* is driven by temperature change and would reflect variations in lake productivity (increasing with warmer water temperatures).

Human impact can be investigated using several palynomorphs. Nitrophilous and ruderal pollen taxa, such as *Convolvulus*, *Plantago lanceolata* type, Urticaceae type and *Polygonum avicularis* type, are often proxies for human impact (Riera et al., 2004), and abundant Amaranthaceae has also been used as well (Sadori et al., 2003). Some species of Cichorioideae have been described as nitrophilous taxa (Abel-Schaad and López-Sáez, 2013) and as grazing indicators (Florenzano et al., 2015; Mercuri et al., 2006; Sadori et al., 2016). At the same time, NPP taxa such as some coprophilous fungi, Sordariales and thecamoebians are also used as indicators of anthropization and land use (Carrión et al., 2007; Ejarque et al., 2015; van Geel et al., 1989; Riera et al., 2006). *Tilletia* a grass-parasitizing fungi has been described as an indicator of grass cultivation in other Iberian records (Carrión et al., 2001a). In this study we follow the example of others (van Geel et al., 1989; Morellón et al., 2016; Sadori et al., 2016) who used the NPP soil mycorrhizal fungus *Glomus* sp. as a proxy for erosive activity.

The palynological analysis, variations in the lithology, geochemistry and macrofossil remains (gastropod shells and charophytes) from the Padul-15-05 core helped us reconstruct the estimated lake level and the local environment changes in the Padul area and their relationship with regional climate (Fig. 5). Several previous studies on Late Holocene lake records from the Iberian Peninsula show that lithological changes can be used as a proxy for lake level reconstruction (Martín-Puertas et al., 2011; Morellón et al., 2009; Riera et al., 2004). For example, carbonate sediments formed by biogenic remains of gastropods and charophytes are indicative of shallow lake waters (Riera et al., 2004). Furthermore, van Geel et al. (1983), described occurrences of *Mougeotia* and *Zygnema* type (Zygnemataceae) as typical of shallow water environments. The increase in organic matter accumulation deduced by TOC (and Br) could be considered as characteristic of high productivity (Kalugin et al., 2007) in these shallow water environments. On the other hand, increases in clastic input in lake sediments have been interpreted as due to lowering of lake level and more influence of terrestrial-fluvial deposition in a very shallow/ephemeral lake (Martín-Puertas et al., 2008). Carrión (2002) related the increase in some fungal species and Asteraceae as indicators of seasonal desiccation stages in lakes. Nevertheless, in natural environments with potential interactions with human activities the increase in clastic deposition related with other indications of soil erosion (e.g. *Glomus* sp.) may be assigned to intensification in land use (Morellón et al., 2016; Sadori et al., 2016).

5.1 Late Holocene aridification trend

Our work confirms the progressive aridification trend that occurred during at least the last ~4700 cal yr BP in the southern Iberian Peninsula, as shown here by the progressive decrease in Mediterranean forest component and the increase in herbs (Figs. 4 and 6). Our lake level interpretations agree with the pollen data, showing an overall decrease during the Late

Holocene, from a shallow water table containing relatively abundant organic matter (high TOC, indicating higher productivity), gastropods and charophytes (high Ca values) to a low-productive ephemeral/emerged environment (high clastic input and MS and decrease in Ca) (Fig. 5). This natural progressive aridification confirmed by the decrease in Mediterranean forest taxa and increase in siliciclastics pointing to a change towards ephemeral (even emerged) environments became more prominent since about 1550 cal yr BP and then enhanced again since ca. 400 cal yr BP to Present. A clear increase in human land use is also observed during the last ca. 1550 cal yr BP (see bellow), including abundant *Glomus* from erosion, which shows that humans were at least partially responsible for this sedimentary change.

A suite of proxies previous studies supports our conclusions regarding the aridification trend since the Middle Holocene (Carrión, 2002; Carrión et al., 2010; Fletcher et al., 2013; Fletcher and Sánchez-Goñi, 2008; Jiménez-Espejo et al., 2014; Jiménez-Moreno et al., 2015). In the western Mediterranean region the decline in forest development during the Middle and Late Holocene is related with a decrease in summer insolation (Fletcher et al., 2013; Jiménez-Moreno and Anderson, 2012), which may have decreased winter rainfall as a consequence of a northward shift of the westerlies - a long-term enhanced positive NAO trend – which induced drier conditions in this area since 6000 cal yr BP (Magny et al., 2012). Furthermore, the decrease in summer insolation would produce a progressive cooling, with a reduction in the length of the growing season as well as a decrease in the sea-surface temperature (Marchal et al., 2002), generating a decrease in the land-sea contrast that would be reflected in a reduction of the wind system and a reduced precipitation gradient from sea to shore during the fall-winter season. The aridification trend can clearly be seen in the nearby alpine records from the Sierra Nevada, where there was little influence by human activity (Anderson et al., 2011; Jiménez-Moreno et al., 2013; Jiménez-Moreno and Anderson, 2012; Ramos-Román et al., 2016).

5.2 Millennial- and centennial-scale climate variability in the Padul area during the Late Holocene

The multi-proxy paleoclimate record from Padul-15-05 shows an overall aridification trend. However, this trend seems to be modulated by millennial- and centennial-scale climatic variability.

5.2.1 Aridity pulses around 4200 (4500, 4300 and 4000 cal yr BP) and around 3000 cal yr BP (3300 and 2800 cal yr BP)

Marked aridity pulses are registered in the Padul-15-05 record around 4200 and 3000 cal yr BP (Unit 1; PA-1 an PA-2a; Figs. 5 and 6). These arid pulses are mostly evidenced in this record by declines in Mediterranean forest taxa, as well as lake level drops and/or cooling evidenced by a decrease in organic component as TOC and the decrease in *Botryococcus* algae. However, a discrepancy between the local and regional occurs between 3000-2800 cal yr BP, with an increase in the estimated lake level and a decrease in the Mediterranean forest during the late Bronze Age until the early Iron Age (Figs. 5 and 6). The disagreement could be due to deforestation by humans during a very active period of mining in the area observed as a peak in lead pollution in the alpine records from Sierra Nevada (García-Alix et al., 2013). The aridity pulses agree regionally with recent studies carried out at higher in elevation in the Sierra Nevada, a decrease in AP percentage in Borreguil de la Caldera record around 4000-3500 cal yr BP (Ramos-Román et al., 2016), high percentage of non-arboreal pollen around 3400 cal ka BP in Zoñar lake [Southern Córdoba Natural Reserve; (Martín-

516   Puertas et al., 2008)], and lake desiccation at ca. 4100 and 2900 cal yr BP in Lake Siles
517   (Carrión et al., 2007). Jalut et al. (2009) compared paleoclimatic records from different lakes
518   in the western Mediterranean region and also suggested a dry phase between 4300 to 3400 cal
519   yr BP, synchronous with this aridification phase. Furthermore, in the eastern Mediterranean
520   basin other pollen studies show a decrease in arboreal pollen concentration toward more open
521   landscapes around 4 cal ka BP (Magri, 1999).
522
523   Significant climatic changes also occurred in the Northern Hemisphere at those times and
524   polar cooling and tropical aridity are observed at ca. 4200-3800 and 3500-2500 cal yr BP;
525   (Mayewski et al., 2004), cold events in the North Atlantic [cold event 3 and 2; (Bond et al.,
526   2001)], decrease in solar irradiance (Steinhilber et al., 2009) and humidity decreases in the
527   eastern Mediterranean area at 4200 cal yr BP (Bar-Matthews et al., 2003) that could be
528   related with global scale climate variability (Fig. 6). These generally dry phases between 4.5
529   and 2.8 in Padul-15-05 are generally in agreement with persistent positive NAO conditions
530   during this time (Olsen et al., 2012).
531   The high-resolution Padul-15-05 record shows that climatic crises such as the essentially
532   global event at~4200 cal yr BP (Booth et al., 2005), are actually multiple events in climate
533   variability at centennial-scales (i.e., ca. 4500, 4300, 4000 cal yr BP).

534 **5.2.2 Iberian-Roman Humid Period (~2600 to 1600 cal yr BP)**

535   High relative humidity is recorded in the Padul-15-05 record between ca. 2600 and 1600 cal
536   yr BP, synchronous with the well-known Iberian-Roman Humid Period (IRHP; between 2600
537   and 1600 cal yr BP; (Martín-Puertas et al., 2009). This is interpreted in our record due to an
538   increase in the Mediterranean forest species at that time (Unit 1; PA-2b; Figs. 6). In addition,
539   there is a simultaneous increase in *Botryococcus* algae, which is probably related to higher
540   productivity during warmer conditions and relatively higher water level. A minimum in
541   sedimentary rates at this time is also recorded, probably related with lower detritic input
542   caused by less erosion due to afforestation and probably also related to the decrease in TOC
543   due to less organic accumulation in the sediment. Evidence of a wetter climate around this
544   period has also been shown in several alpine records from Sierra Nevada. For example, in the
545   Laguna de la Mula core (Jiménez-Moreno et al. 2013) an increase in deciduous *Quercus* is
546   correlated with the maximum in algae between 2500 to 1850 cal yr BP, also evidencing the
547   most humid period of the Late Holocene. A geochemical study from the Laguna de Río Seco
548   (also in Sierra Nevada) also evidenced humid conditions around 2200 cal yr BP by the
549   decrease in Saharan dust input and the increase in detritic sedimentation into the lake
550   suggesting higher rainfall (Jiménez-Espejo et al., 2014). In addition, Ramos-Román et al.
551   (2016) showed an increase in AP in the Borreguil de la Caldera record around 2200 cal yr
552   BP, suggesting an increase in humidity at that time.
553
554   Other records from the Iberian Peninsula also show this pattern to wetter conditions during
555   the IRHP. For example, high lake levels are recorded in Zoñar Lake in southern Spain
556   between 2460 to 1600 cal yr BP, only interrupted by a relatively arid pulse between 2140 and
557   1800 cal yr BP (Martín-Puertas et al., 2009). An increase in rainfall is described in the central
558   region of the Iberian Peninsula in a study from the Tablas de Daimiel National Park between
559   2100 and 1680 cal yr BP (Gil García et al., 2007). Deeper lake levels at around 2650 to 1580
560   cal yr BP, also interrupted by an short arid event at ca. 2125-1790 cal yr BP, were observed
561   to the north, in the Iberian Range (Currás et al., 2012). The fact that the Padul-15-05 record
562   also shows a relatively arid-cold event between 2150-2050 cal yr BP, just in the middle of
563   this relative humid-warm period, seems to point to a common feature of centennial-scale

566 climatic variability in many western Mediterranean and North Atlantic records (Fig. 6).
567 Humid climate conditions at around 2500 cal yr BP are also interpreted in previous studies
568 from lake level reconstructions from Central Europe (Magny, 2004). Increases in temperate
569 deciduous forest are also observed in marine records from the Alboran Sea around 2600 to
570 2300 cal yr BP, also pointing to high relative humidity (Combourieu-Nebout et al., 2009).
571 Overall humid conditions between 2600 and 1600 cal yr BP seem to agree with predominant
572 negative NAO reconstructions at that time, which would translate into greater winter (and
573 thus more effective) precipitation in the area triggering greater development of forest species
574 in the area.
575
576 Generally warm conditions are interpreted between 1900 and 1700 cal yr BP in the
577 Mediterranean Sea, with high sea surface temperatures (SSTs), and in the North Atlantic
578 area, with the decrease in Drift Ice Index. In addition, persistent positive solar irradiance
579 occurred at that time. The increase in *Botryococcus* algae reaching maxima during the IRHP
580 also seems to point to very productive and perhaps warmer conditions in the Padul area (Fig.
581 6). There seems to be a short lag of about 200 years between maximum in *Botryococcus* and
582 maximum in Mediterranean forest. This could be due to different speed of reaction to climate
583 change, with algae (short life cycle, blooming if conditions are favorable) responding faster
584 than forest (tree development takes decades). An alternative explanation could be that they
585 might be responding to different forcings, with regional signal (forest) mostly conditioned by
586 precipitation and local (algae) also conditioned by temperature (productivity).

5.2.3 DA and MCA (~1550 cal yr BP to 600 cal yr BP)

588 Enhanced aridity occurred right after the IRHP in the Padul area. This is deduced in the
589 Padul-15-05 record by a significant forest decline, with a prominent decrease in
590 Mediterranean forest elements, an increase in herbs (Unit 1; PA-3; Figs. 4 and 6). In addition,
591 our evidence suggests a transition from a shallow lake to a more ephemeral wetland. This is
592 suggested by the disappearance of charophytes, a significant decrease in algae component
593 and higher Si and MS and lower TOC values (Unit 1; Figs. 5). Humans probably also
594 contributed to enhancing erosion in the area during this last ~1550 cal yr BP. The significant
595 change during the transition from Unit 1 to Unit 2 with a decrease in the pollen concentration
596 and the increase in Cichoroideae could be due to enhanced pollen degradation as
597 Cichoroideae have been found to be very resistant to pollen deterioration (Bottema, 1975).
598 However, the occurrence of other pollen taxa (e.g. *Quercus*, Ericaceae, *Pinus*, Poaceae, *Olea*)
599 showing climatic trends and increasing between ca. 1500-400 cal yr BP and a decrease in
600 Cichoroideae in the last ~400 cal yr BP, when an increase in clastic material occurred, do not
601 entirely support a preservation issue (see section of Human activity; 5.4).
602
603 This phase could be separated into two different periods. The first period occurred between
604 ~1550 cal yr BP and 1100 cal yr BP (~400 to 900 CE) and is characterized by a decreasing
605 trend in Mediterranean forest and *Botryococcus* taxa. This period corresponds with the Dark
606 Ages [from ca. 500 to 900 CE; (Moreno et al., 2012)]. Correlation between the decline in
607 Mediterranean forest, the increase in the Drift Ice Index in the North Atlantic record (cold
608 event 1; Bond et al., 2001), the decline in SSTs in the Mediterranean Sea and maxima in
609 positive NAO reconstructions suggests drier and colder conditions during this time (Fig. 6).
610 Other Mediterranean and central-European records agree with our climate interpretations, for
611 example, a decrease in forest pollen types is shown in a marine record from the Alboran Sea
612 (Fletcher et al., 2013) and a decrease in lake levels is also observed in Central Europe
613 (Magny et a., 2004) pointing to aridity during the DA. Evidences of aridity during the DA

have been shown too in the Mediterranean part of the Iberian Peninsula, for instance, cold and arid conditions were suggested in the northern Betic Range by the increase in xerophytic herbs around 1450 and 750 cal yr BP (Carrión et al., 2001b) and in southeastern Spain by a forest decline in lacustrine deposits around 1620 and 1160 cal yr BP (Carrión et al., 2003). Arid and colder conditions during the Dark Ages (around 1680 to 1000 cal yr BP) are also suggested for the central part of the Iberian Peninsula using a multiproxy study of a sediment record from the Tablas de Daimiel Lake (Gil García et al., 2007).

A second period that we could differentiate occurred around 1100 to 600 cal yr BP/900 to 1350 CE, during the well-known MCA (900 to 1300 CE after Moreno et al., 2012). During this period the Padul-15-05 record shows a slight increasing trend in the Mediterranean forest taxa with respect to the DA, but the decrease in *Botryococcus* and the increase in herbs still point to overall arid conditions. This change could be related to an increase in temperature, favoring the development of temperate forest species, and would agree with inferred increasing temperatures in the North Atlantic areas, as well as the increase in solar irradiance and the increase in SSTs in the Mediterranean Sea (Fig. 6). This hypothesis would agree with the reconstruction of persistent positive NAO and overall warm conditions during the MCA in the western Mediterranean (see synthesis in Moreno et al., 2012). A similar pattern of increasing xerophytic vegetation during the MCA is observed in alpine peat bogs and lakes in the Sierra Nevada (Anderson et al., 2011; Jiménez-Moreno et al., 2013; Ramos-Román et al., 2016) and arid conditions are shown to occur during the MCA in southern and eastern Iberian Peninsula deduced by increases in salinity and lower lake levels (Corella et al., 2013; Martín-Puertas et al., 2011). However, humid conditions have been reconstructed for the northwestern of the Iberian Peninsula at this time (Lebreiro et al., 2006; Moreno et al., 2012), as well as northern Europe (Martín-Puertas et al., 2008). The different pattern of precipitation between northwestern Iberia / northern Europe and the Mediterranean area is undoubtedly a function of the NAO precipitation dipole (Trouet et al., 2009).

5.2.4 The last ~600 cal yr BP: LIA (~600 to 100 cal yr BP/~1350 to1850 CE) and IE (~100 cal yr BP to Present/~1850 CE-Present)

Two climatically distinct periods can be distinguished during the last ca. 600 years (end of PA-3b to PA-4; Fig. 4) in the area. However, the climatic signal is more difficult to interpret due to a higher human impact at that time. The first phase around 600-500 cal yr BP was characterized as increasing relative humidity by the decrease in xerophytes and the increase in Mediterranean forest taxa and *Botryococcus* after a period of decrease during the DA and MCA, corresponding to the LIA. The second phase is characterized here by the decrease in the Mediterranean forest around 300-100 cal yr BP, pointing to a return to more arid conditions during the last part of the LIA (Figs. 5 and 6). This climatic pattern agrees with an increase in precipitation by the transition from positive to negative NAO mode and from warmer to cooler conditions in the North Atlantic area during the first phase of the LIA and a second phase characterized by cooler (cold event 0; Bond et al., 2001) and drier conditions (Fig. 6). A stronger variability in the SSTs is described in the Mediterranean Sea during the LIA (Fig. 6). Mayewski et al. (2004) described a period of climate variability during the Holocene at this time (600 to 150 cal yr BP) suggesting a polar cooling but more humid in some parts of the tropics. Regionally, (Morellón et al., 2011) also described a phase of more humid conditions between 1530 to 1750 CE (420 to 200 cal yr BP) in a lake sediment record from NE Spain. An alternation between wetter to drier periods during the LIA are also shown in the nearby alpine record from Borreguil de la Caldera in the Sierra Nevada mountain range (Ramos-Román et al., 2016).

664 The environmental transition from ephemeral, observed in the last ca. 1550 cal yr BP (Unit 1;
665 Fig. 5), to emerged conditions occur in the last ca. 400 cal yr BP. This is shown by the
666 highest MS and Si values, enhance sedimentation rates and the increase in wetland plants and
667 the stronger decrease in Ca and organic components (TOC) in the sediments in the uppermost
668 part of the Padul-15-05 record (Unit 2; Figs. 3 and 5).

669 **5.3 Centennial-scale variability**

670 Time series analysis has become important in determining the recurrent periodicity of
671 cyclical oscillations in paleoenvironmental sequences (e.g. Jiménez-Espejo et al., 2014;
672 Ramos-Román et al., 2016; Rodrigo-Gámiz et al., 2014; Fletcher et al., 2013). This analysis
673 also assists in understanding possible relationships between the paleoenvironmental proxy
674 data and the potential triggers of the observed cyclical changes: i.e., solar activity,
675 atmospheric, oceanic dynamics and climate evolution during the Holocene. The
676 cyclostratigraphic analysis on the pollen (Mediterranean forest; regional signal), algae
677 (*Botryococcus*; local signal) and TOC (local signal) times series from the Padul-15-05 record
678 evidence centennial-scale cyclical patterns with periodicities around ~800, 680, 300, 240, 200
679 and 170 years above the 90 % confidence levels (Fig. 7).
680
681 Previous cyclostratigraphic analysis in Holocene western Mediterranean records suggest
682 cyclical climatic oscillations with periodicities around 1500 and 1750 yr (Fletcher et al.,
683 2013; Jiménez-Espejo et al., 2014; Rodrigo-Gámiz et al., 2014). Other North Atlantic and
684 Mediterranean records also present cyclicities in their paleoclimatic proxies of ca. 1600 yr
685 (Bond et al., 2001; Debret et al., 2007; Rodrigo-Gámiz et al., 2014). However, this cycle is
686 absent from the cyclostratigraphic analysis in the Padul-15-05 record (Fig. 7). In contrast, the
687 spectral analysis performed in the Mediterranean forest time series from Padul record,
688 pointing to cyclical hydrological changes, shows a significant ~800 yr cycle that could be
689 related to solar variability (Damon and Sonett, 1991) or could be the second harmonic of the
690 ca. ~1600 yr oceanic-related cycle (Debret et al., 2009). A very similar periodicity of ca. 760
691 yr is detected in the *Pinus* forest taxa, also pointing to humidity variability, from the alpine
692 Sierra Nevada site of Borreguil de la Caldera and seems to show that this is a common
693 feature of cyclical paleoclimatic oscillation in the area.
694
695 A significant ~680 cycle is shown in the *Botryococcus* time series most likely suggesting
696 recurrent centennial-scale changes in temperature (productivity) and water availability. A
697 similar cycle is shown in the *Artemisia* signal in an alpine record from Sierra Nevada
698 (Ramos-Román et al., 2016). This cycle around ~650 yr is also observed in a marine record
699 from the Alboran Sea, and was interpreted as the secondary harmonic of the 1300 yr cycle
700 that those authors related with cyclic thermohaline circulation and sea surface temperature
701 changes (Rodrigo-Gámiz et al., 2014).
702
703 A statistically significant ~300 yr cycle is shown in the Mediterranean forest taxa and TOC
704 from the Padul-15-05 record suggesting shorter-scale variability in water availability. This
705 cycle is also observed in the cyclical *Pinus* pollen data from Borreguil de la Caldera at higher
706 elevations in the Sierra Nevada (Ramos-Román et al., 2016). This cycle could be principally
707 related to NAO variability as observed by Olsen et al. (2012), which follows variations in
708 humidity observed in the Padul-15-05 record. NAO variability also regulates modern
709 precipitation in the area.
710
711 The *Botryococcus* and TOC time series shows variability with a periodicity around ~240, 200

and 164 yrs. Sonett and Suess, (1984) described a significant cycle in solar activity around
~208 yr (Suess solar cycle), which could have triggered our ~200 cyclicity. The observed
~240 yr periodicity in the Padul-15-05 record could be either related to variations in solar
activity or due to the mixed effect of the solar together with the ~300 yr NAO-interpreted
cycle and could point to a solar origin of the centennial-scale NAO variations as suggested by
previously published research (Lukianova and Alekseev, 2004; Zanchettin et al., 2008).
Finally, a significant ~170 yr cycle has been observed in both the Mediterranean forest taxa
and *Botryococcus* times series from the Padul-15-05 record. A similar cycle (between 168-
174 yr) was also described in the alpine pollen record from Borreguil de la Caldera in Sierra
Nevada (Ramos-Román et al., 2016), which shows that it is a significant cyclical pattern in
climate, probably precipitation, in the area. This cycle could be related to the previously
described ~170 yr cycle in the NAO index (Olsen et al., 2012), which would agree with the
hypothesis of the NAO controlling millennial- and centennial-scale environmental variability
during the Late Holocene in the area (García-Alix et al., 2017; Ramos-Román et al., 2016).

5.4 Human activity

Humans probably had an impact in the area since Prehistoric times, however, the Padul-15-05
multiproxy record shows a more significant human impact during the last ca. 1550 cal yr BP,
which intensified in the last ~500 years (since 1450 CE to Present). This is deduced by, a
significant increase in nitrophilous plant taxa such as Cichorioideae, Convolvulaceae,
Polygonaceae and *Plantago* and the increase in some NPP such as *Tilletia*, coprophilous
fungi and thecamoebians (Unit 2; PA-4; Fig. 4). Most of these pollen taxa and NPPs are
described in other southern Iberian paleoenvironmental records as indicators of land uses, for
instance, *Tilletia* and covarying nitrophilous plants have been described as indicators of
farming (e.g. Carrión et al., 2001a). Thecamoebians also show a similar trend and have also
been detected in other areas being related to nutrient enrichment as consequences of livestock
(Fig. 8). The stronger increase in Cichorioideae have also been described as indicators of
animal grazing in areas subjected to intense use of the territory (Mercuri et al., 2006).
Interestingly, these taxa began to decline around ca. 400 cal yr BP (~1550 CE), coinciding
with the higher increase in detritic material into the basin. We could then interpreted this
increase in Cichorioideae as greater in livestock activity in the surroundings of the lake
during this period, which is supported by the increase in these other proxies related with
animal husbandry.

Climatically, this event coincides with the start of persistent negative NAO conditions in the
area (Trouet et al., 2009), which could have further triggered more rainfall and more detritic
input into the basin. (Bellin et al., 2011) in a study from the Betic Cordillera (southern Iberian
Peninsula) demonstrate that soil erosion increase in years with higher rainfall and this could
be intensified by human impact. Nevertheless, in a study in the southeastern part of the
Iberian Peninsula (Bellin et al., 2013) suggested that major soil erosion could have occurred
by the abandonment of agricultural activities in the mountain areas as well as the
abandonment of irrigated terrace systems during the Christian Reconquest. Enhanced soil
erosion at this time is also supported by the increase in *Glomus* type (Figs. 4 and 8).

An important change in the sedimentation in the environment is observed during the last ca.
400 cal yr BP marked by the stronger increase in MS and Si values. This higher increase in
detritics occurred during an increase in other plants related with human and land uses such as
Polygonaceae, Amaranthaceae, Convolvulaceae, *Plantago*, Apiaceae and Cannabaceae-
Urticaceae type (Land Use Plants; Fig. 8). This was probably related to drainage canals in the

761 Padul wetland in the late XVIII century for cultivation purposes (Villegas Molina, 1967). The
762 increase in wetland vegetation and higher values of Poaceae could be due to cultivation of
763 cereals or by an increase in the population of *Phragmites australis* (also a Poaceae), very
764 abundant in the Padul lake margins at present due to the increase in drained land surface.
765 The uppermost part (last ca. 100 cal yr BP) of the pollen record from Padul-15-05 shows an
766 increasing trend in some arboreal taxa at that time, including Mediterranean forest, *Olea* and
767 *Pinus* (Fig. 4). This change is most likely of human origin and generated by the increase in
768 *Olea* cultivation in the last two centuries, also observed in many records from higher
769 elevation sites from Sierra Nevada, and *Pinus* and other Mediterranean species reforestation
770 in the 20th century (Anderson et al., 2011; Jiménez-Moreno and Anderson, 2012; Jiménez-
771 Moreno et al., 2013; Ramos-Román et al., 2016).

772 **6 Conclusions**

773 Our multiproxy analysis from the Padul-15-05 sequence has provided a detailed climate
774 reconstruction for the last 4700 ca yr BP for the Padul area and the western Mediterranean.
775 This study, supported by the comparison with other Mediterranean and North Atlantic
776 records suggests a link between vegetation, atmospheric dynamics and insolation and solar
777 activity during the Late Holocene. A climatic aridification trend occurred during the Late
778 Holocene in the Sierra Nevada and the western Mediterranean, probably linked with an
779 orbital-scale declining trend in summer insolation. This long-term trend is modulated by
780 centennial-scale climate variability as shown by the pollen (Mediterranean forest taxa), algae
781 (*Botryococcus*) and sedimentary and geochemical data in the Padul record. These events can
782 be correlated with regional and global scale climate variability. Cold and arid pulses
783 identified in this study around the 4200 and 3000 cal yr BP are synchronous with cold events
784 recorded in the North Atlantic and decreases in precipitation in the Mediterranean area,
785 probably linked to persistent positive NAO mode. Moreover, one of the most important
786 humid and warmer periods during the Late Holocene in the Padul area coincides in time with
787 the well-known IRHP, characterized by warm and humid conditions in the Mediterranean and
788 North Atlantic regions and overall negative NAO conditions. A drastic decline in
789 Mediterranean forest taxa, trending towards an open landscape and pointing to colder
790 conditions with enhanced aridity, occurred in two steps (DA and end of the LIA) during the
791 last ~1550 cal yr BP. However, this trend was slightly superimposed by a more arid but
792 warmer event coinciding with the MCA and a cold but wetter event during the first part of the
793 LIA. Besides natural climatic and environmental variability, strong evidences exists for
794 intense human activities in the area during the last ~1550 years. This suggests that the natural
795 aridification trend during the Late Holocene, which produced a progressive decrease in the
796 Mediterranean forest taxa in the Padul area, could have been intensified by human activities,
797 notably in the last centuries.
798 Furthermore, time series analyses done in the Padul-15-05 record show centennial-scale
799 changes in the environment and climate that are coincident with the periodicities observed in
800 solar, oceanic and NAO reconstructions and could show a close cause-and-effect linkage
801 between them.

802 **Acknowledgements**

803 This work was supported by the project P11-RNM-7332 funded by Consejería de Economía,
804 Innovación, Ciencia y Empleo de la Junta de Andalucía, the project CGL2013-47038-R
805 funded by Ministerio de Economía y Competitividad of Spain and fondo Europeo de
806 desarrollo regional FEDER and the research group RNM0190 (Junta de Andalucía). M. J. R.-
807 R. acknowledges the PhD funding provided by Consejería de Economía, Innovación, Ciencia

812 y Empleo de la Junta de Andalucía (P11-RNM-7332). J.C. acknowledges the PhD funding
813 provided by Ministerio de Economía y Competitividad (CGL2013-47038-R). A.G.-A. was
814 also supported by a Ramón y Cajal Fellowship RYC-2015-18966 of the Spanish Government
815 (Ministerio de Economía y Competividad). Javier Jaimez (CIC-UGR) is thanked for
816 graciously helping with the coring, the drilling equipment and logistics. We also would like
817 to thanks to the editor (Nathalie Combourieu-Nebout) and Graciela Gil-Romera, Laura
818 Sadori and an anonymous reviewer for their comments and suggestions which improved the
819 manuscript.

820

References

Abel-Schaad, D. and López-Sáez, J. A.: Vegetation changes in relation to fire history and human activities at the Peña Negra mire (Bejar Range, Iberian Central Mountain System, Spain) during the past 4,000 years, Veg. Hist. Archaeobotany, 22(3), 199–214, doi:10.1007/s00334-012-0368-9, 2013.

Alfaro, P., Galinod-Zaldievar, J., Jabaloy, A., López-Garrido, A. C. and Sanz de Galdeano, C.: Evidence for the activity and paleoseismicity of the Padul fault (Betic Cordillera, Southern Spain) [Evidencias de actividad y paleosismicidad de la falla de Padul (Cordillera Bética, sur de España)], Acta Geol. Hisp., 36(3–4), 283–297, 2001.

Alpert, P., Baldi, M., Ilani, R., Krichak, S., Price, C., Rodó, X., Saaroni, H., Ziv, B., Kishcha, P., Barkan, J., Mariotti, A. and Xoplaki, E.: Chapter 2 Relations between climate variability in the Mediterranean region and the tropics: ENSO, South Asian and African monsoons, hurricanes and Saharan dust, Dev. Earth Environ. Sci., 4(C), 149–177, doi:10.1016/S1571-9197(06)80005-4, 2006.

Anderson, R. S., Jiménez-Moreno, G., Carrión, J. S. and Pérez-Martínez, C.: Postglacial history of alpine vegetation, fire, and climate from Laguna de Río Seco, Sierra Nevada, southern Spain, Quat. Sci. Rev., 30(13–14), 1615–1629, doi:https://doi.org/10.1016/j.quascirev.2011.03.005, 2011.

Bar-Matthews, M., Ayalon, A., Gilmour, M., Matthews, A. and Hawkesworth, C. J.: Sea–land oxygen isotopic relationships from planktonic foraminifera and speleothems in the Eastern Mediterranean region and their implication for paleorainfall during interglacial intervals, Geochim. Cosmochim. Acta, 67(17), 3181–3199, doi:https://doi.org/10.1016/S0016-7037(02)01031-1, 2003.

Bellin, N., Vanacker, V., van Wesemael, B., Solé-Benet, A. and Bakker, M. M.: Natural and anthropogenic controls on soil erosion in the internal betic Cordillera (southeast Spain), Catena, 87(2), 190–200, doi:10.1016/j.catena.2011.05.022, 2011.

Bellin, N., Vanacker, V. and De Baets, S.: Anthropogenic and climatic impact on Holocene sediment dynamics in SE Spain: A review, Quat. Int., 308–309, 112–129, doi:10.1016/j.quaint.2013.03.015, 2013.

Beug, H.-J.: Leitfaden der Pollenbestimmung für Mitteleuropa und angrenzende Gebiete, Fisch. Stuttg., 61, 2004.

Blaauw, M.: Methods and code for 'classical' age-modelling of radiocarbon sequences, Quat. Geochronol., 5(5), 512–518, doi:https://doi.org/10.1016/j.quageo.2010.01.002, 2010.

Bond, G., Kromer, B., Beer, J., Muscheler, R., Evans, M. N., Showers, W., Hoffmann, S., Lotti-Bond, R., Hajdas, I. and Bonani, G.: Persistent Solar Influence on North Atlantic Climate During the Holocene, Science, 294(5549), 2130, doi:10.1126/science.1065680, 2001.

Booth, R. K., Jackson, S. T., Forman, S. L., Kutzbach, J. E., E. A. Bettis, I., Kreigs, J. and Wright, D. K.: A severe centennial-scale drought in midcontinental North America 4200

860 years ago and apparent global linkages, The Holocene, 15(3), 321–328,
861 doi:10.1191/0959683605hl825ft, 2005.

862 Bottema, S.: The interpretation of pollen spectra from prehistoric settlements (with special
863 attention of Liguliflorae), Palaeohistoria, 17, 17–35, 1975.

864 Carrión, J. S.: Patterns and processes of Late Quaternary environmental change in a montane
865 region of southwestern Europe, Quat. Sci. Rev., 21(18–19), 2047–2066,
866 doi:https://doi.org/10.1016/S0277-3791(02)00010-0, 2002.

867 Carrión, J. S., Munuera, M., Dupré, M. and Andrade, A.: Abrupt vegetation changes in the
868 Segura Mountains of southern Spain throughout the Holocene, J. Ecol., 89(5), 783–797,
869 doi:10.1046/j.0022-0477.2001.00601.x, 2001b.

870 Carrión, J. S., Andrade, A., Bennett, K. D., Navarro, C. and Munuera, M.: Crossing forest
871 thresholds: inertia and collapse in a Holocene sequence from south-central Spain, The
872 Holocene, 11(6), 635–653, doi:10.1191/09596830195672, 2001a.

873 Carrión, J. S., Fernández, S., Jiménez-Moreno, G., Fauquette, S., Gil-Romera, G., González-
874 Sampériz, P. and Finlayson, C.: The historical origins of aridity and vegetation degradation in
875 southeastern Spain, J. Arid Environ., 74(7), 731–736,
876 doi:https://doi.org/10.1016/j.jaridenv.2008.11.014, 2010a.

877 Carrión, J. S., Sánchez-Gómez, P., Mota, J. F., Yll, R. and Chaín, C.: Holocene vegetation
878 dynamics, fire and grazing in the Sierra de Gádor, southern Spain, Holocene, 13(6), 839–849,
879 doi:10.1191/0959683603hl662rp, 2003.

880 Carrión, J. S., Fuentes, N., González-Sampériz, P., Quirante, L. S., Finlayson, J. C.,
881 Fernández, S. and Andrade, A.: Holocene environmental change in a montane region of
882 southern Europe with a long history of human settlement, Quat. Sci. Rev., 26(11–12), 1455–
883 1475, doi:https://doi.org/10.1016/j.quascirev.2007.03.013, 2007.

884 Castillo Martín, A., Benavente Herrera, J., Fernández Rubio, R. and Pulido Bosch, A.:
885 Evolución y ámbito hidrogeológico de la laguna de Padul (Granada), Las Zonas Húmedas En
886 Andal. Monogr. DGMA-MOPU, 1984.

887 Combourieu-Nebout, N., Peyron, O., Dormoy, I., Desprat, S., Beaudouin, C., Kotthoff, U.
888 and Marret, F.: Rapid climatic variability in the west Mediterranean during the last 25 000
889 years from high resolution pollen data, Clim Past, 5(3), 503–521, doi:10.5194/cp-5-503-
890 2009, 2009.

891 Corella, J. P., Stefanova, V., El Anjoumi, A., Rico, E., Giralt, S., Moreno, A., Plata-Montero,
892 A. and Valero-Garcés, B. L.: A 2500-year multi-proxy reconstruction of climate change and
893 human activities in northern Spain: The Lake Arreo record, Palaeogeogr. Palaeoclimatol.
894 Palaeoecol., 386, 555–568, doi:10.1016/j.palaeo.2013.06.022, 2013.

895 Currás, A., Zamora, L., Reed, J. M., García-Soto, E., Ferrero, S., Armengol, X., Mezquita-
896 Joanes, F., Marqués, M. A., Riera, S. and Julià, R.: Climate change and human impact in
897 central Spain during Roman times: High-resolution multi-proxy analysis of a tufa lake record
898 (Somolinos, 1280m asl), Catena, 89(1), 31–53, doi:10.1016/j.catena.2011.09.009, 2012.

899 Damon, P. E. and Sonett, C. P.: Solar and terrestrial components of the atmospheric C-14
900 variation spectrum. In: Sonett, C.P., Giampapa, M.S., Matthews, M.S. (Eds.), The Sun in
901 Time. University of Arizona Press, Tucson, AZ, USA., 1991.

902 Debret, M., Bout-Roumazeilles, V., Grousset, F., Desmet, M., McManus, J. F., Massei, N.,
903 Sebag, D., Petit, J.-R., Copard, Y. and Trentesaux, A.: The origin of the 1500-year climate
904 cycles in holocene north-atlantic records, Clim. Past, 3(4), 569–575, 2007.

905 Debret, M., Sebag, D., Crosta, X., Massei, N., Petit, J.-R., Chapron, E. and Bout-
906 Roumazeilles, V.: Evidence from wavelet analysis for a mid-Holocene transition in global
907 climate forcing, Quat. Sci. Rev., 28(25–26), 2675–2688,
908 doi:https://doi.org/10.1016/j.quascirev.2009.06.005, 2009.

909 Delgado, J., Alfaro, P., Galindo-Zaldivar, J., Jabaloy, A., Lopez Garrido, A. and Sanz de
910 Galdeano, C.: Structure of the Padul-Nigüelas basin (S Spain) from H/V ratios of ambient
911 noise: application of the method to study peat and coarse sediments, Pure Appl. Geophys.,
912 159(11), 2733–2749, 2002.

913 Domingo-García, M., Fernández-Rubio, R., Lopez, J. and González, C.: Aportación al
914 conocimiento de la Neotectónica de la Depresión del Padul (Granada), Tecniterrae, 53, 6–16,
915 1983.

916 Ejarque, A., Anderson, R. S., Simms, A. R. and Gentry, B. J.: Prehistoric fires and the
917 shaping of colonial transported landscapes in southern California: A paleoenvironmental
918 study at Dune Pond, Santa Barbara County, Quat. Sci. Rev., 112, 181–196,
919 doi:https://doi.org/10.1016/j.quascirev.2015.01.017, 2015.

920 El Aallali, A., Nieto, J. M. L., Raya, F. A. P. and Mesa, J. M.: Estudio de la vegetación
921 forestal en la vertiente sur de Sierra Nevada (Alpujarra Alta granadina), Itinera Geobot., (11),
922 387–402, 1998.

923 Faegri, K. and Iversen, J.: Textbook of Pollen Analysis. Wiley, New York., 1989.

924 Fletcher, W. J. and Sánchez-Goñi, M. F.: Orbital- and sub-orbital-scale climate impacts on
925 vegetation of the western Mediterranean basin over the last 48,000 yr, Quat. Res., 70(3),
926 451–464, doi:10.1016/j.yqres.2008.07.002, 2008.

927 Fletcher, W. J., Debret, M. and Sánchez-Goñi, M. F.: Mid-Holocene emergence of a low-
928 frequency millennial oscillation in western Mediterranean climate: Implications for past
929 dynamics of the North Atlantic atmospheric westerlies, The Holocene, 23(2), 153–166,
930 doi:10.1177/0959683612460783, 2013.

931 Florenzano, A., Marignani, M., Rosati, L., Fascetti, S. and Mercuri, A. M.: Are Cichorieae an
932 indicator of open habitats and pastoralism in current and past vegetation studies?, Plant
933 Biosyst. - Int. J. Deal. Asp. Plant Biol., 149(1), 154–165,
934 doi:10.1080/11263504.2014.998311, 2015.

935 Florschütz, F., Amor, J. M. and Wijmstra, T. A.: Palynology of a thick quaternary succession
936 in southern Spain, Palaeogeogr. Palaeoclimatol. Palaeoecol., 10(4), 233–264,
937 doi:http://dx.doi.org/10.1016/0031-0182(71)90049-6, 1971.

938 García-Alix, A., Jimenez-Espejo, F. J., Lozano, J. A., Jiménez-Moreno, G., Martinez-Ruiz,
939 F., Sanjuán, L. G., Jiménez, G. A., Alfonso, E. G., Ruiz-Puertas, G. and Anderson, R. S.:
940 Anthropogenic impact and lead pollution throughout the Holocene in Southern Iberia, Sci.
941 Total Environ., 449, 451–460, doi:https://doi.org/10.1016/j.scitotenv.2013.01.081, 2013.

942 García-Alix, A., Jiménez-Espejo, F. J., Toney, J. L., Jiménez-Moreno, G., Ramos-Román, M.
943 J., Anderson, R. S., Ruano, P., Queralt, I., Delgado Huertas, A. and Kuroda, J.: Alpine bogs
944 of southern Spain show human-induced environmental change superimposed on long-term
945 natural variations, Sci. Rep., 7(1), 7439, doi:10.1038/s41598-017-07854-w, 2017.

946 van Geel, B., Hallewas, D. P. and Pals, J. P.: A late holocene deposit under the Westfriese
947 Zeedijk near Enkhuizen (Prov. of Noord-Holland, The Netherlands): Palaeoecological and
948 archaeological aspects, Rev. Palaeobot. Palynol., 38(3), 269–335,
949 doi:http://dx.doi.org/10.1016/0034-6667(83)90026-X, 1983.

950 van Geel, B., Coope, G. R. and Hammen, T. V. D.: Palaeoecology and stratigraphy of the
951 lateglacial type section at Usselo (the Netherlands), Rev. Palaeobot. Palynol., 60(1), 25–129,
952 doi:http://dx.doi.org/10.1016/0034-6667(89)90072-9, 1989.

953 Gil García, M. J., Ruiz Zapata, M. B., Santisteban, J. I., Mediavilla, R., López-Pamo, E. and
954 Dabrio, C. J.: Late holocene environments in Las Tablas de Daimiel (south central Iberian
955 peninsula, Spain), Veg. Hist. Archaeobotany, 16(4), 241–250, doi:10.1007/s00334-006-0047-
956 9, 2007.

957 Gil-Romera, G., Carrión, J. S., Pausas, J. G., Sevilla-Callejo, M., Lamb, H. F., Fernández, S.
958 and Burjachs, F.: Holocene fire activity and vegetation response in South-Eastern Iberia,
959 Quat. Sci. Rev., 29(9), 1082–1092, doi:10.1016/j.quascirev.2010.01.006, 2010.

960 Grimm, E. C.: CONISS: a FORTRAN 77 program for stratigraphically constrained cluster
961 analysis by the method of incremental sum of squares, Comput. Geosci., 13(1), 13–35,
962 doi:http://dx.doi.org/10.1016/0098-3004(87)90022-7, 1987.

963 Guy-Ohlson, D.: Botryococcus as an aid in the interpretation of palaeoenvironment and
964 depositional processes, Rev. Palaeobot. Palynol., 71(1), 1–15,
965 doi:http://dx.doi.org/10.1016/0034-6667(92)90155-A, 1992.

966 Hurrell, J. W.: Decadal Trends in the North Atlantic Oscillation: Regional Temperatures and
967 Precipitation, Science, 269(5224), 676, doi:10.1126/science.269.5224.676, 1995.

968 Jalut, G., Dedoubat, J. J., Fontugne, M. and Otto, T.: Holocene circum-Mediterranean
969 vegetation changes: Climate forcing and human impact, Quat. Int., 200(1–2), 4–18,
970 doi:https://doi.org/10.1016/j.quaint.2008.03.012, 2009.

971 Jiménez-Espejo, F. J., García-Alix, A., Jiménez-Moreno, G., Rodrigo-Gámiz, M., Anderson,
972 R. S., Rodríguez-Tovar, F. J., Martínez-Ruiz, F., Giralt, S., Delgado Huertas, A. and Pardo-
973 Igúzquiza, E.: Saharan aeolian input and effective humidity variations over western Europe
974 during the Holocene from a high altitude record, Chem. Geol., 374–375, 1–12,
975 doi:10.1016/j.chemgeo.2014.03.001, 2014.

976 Jiménez-Moreno, G. and Anderson, R. S.: Holocene vegetation and climate change recorded
977 in alpine bog sediments from the Borreguiles de la Virgen, Sierra Nevada, southern Spain,
978 Quat. Res., 77(1), 44–53, doi:10.1016/j.yqres.2011.09.006, 2012.

979 Jiménez-Moreno, G., García-Alix, A., Hernández-Corbalán, M. D., Anderson, R. S. and
980 Delgado-Huertas, A.: Vegetation, fire, climate and human disturbance history in the
981 southwestern Mediterranean area during the late Holocene, Quat. Res., 79(2), 110–122,
982 doi:https://doi.org/10.1016/j.yqres.2012.11.008, 2013.

983 Jiménez-Moreno, G., Rodríguez-Ramírez, A., Pérez-Asensio, J. N., Carrión, J. S., López-
984 Sáez, J. A., Villarías-Robles, J. J. R., Celestino-Pérez, S., Cerrillo-Cuenca, E., León, Á. and
985 Contreras, C.: Impact of late-Holocene aridification trend, climate variability and
986 geodynamic control on the environment from a coastal area in SW Spain, Holocene, 25(4),
987 607–617, doi:10.1177/0959683614565955, 2015.

988 Kalugin, I., Daryin, A., Smolyaninova, L., Andreev, A., Diekmann, B. and Khlystov, O.:
989 800-yr-long records of annual air temperature and precipitation over southern Siberia inferred
990 from Teletskoye Lake sediments, Quat. Res., 67(3), 400–410,
991 doi:https://doi.org/10.1016/j.yqres.2007.01.007, 2007.

992 Laskar, J., Robutel, P., Joutel, F., Gastineau, M., Correia, A. C. M. and Levrard, B.: A long-
993 term numerical solution for the insolation quantities of the Earth, A&A, 428(1), 261–285,
994 doi:10.1051/0004-6361:20041335, 2004.

995 Lebreiro, S. M., Francés, G., Abrantes, F. F. G., Diz, P., Bartels-Jónsdóttir, H. B.,
996 Stroynowski, Z. N., Gil, I. M., Pena, L. D., Rodrigues, T., Jones, P. D., Nombela, M. A.,
997 Alejo, I., Briffa, K. R., Harris, I. and Grimalt, J. O.: Climate change and coastal hydrographic
998 response along the Atlantic Iberian margin (Tagus Prodelta and Muros Ría) during the last
999 two millennia, Holocene, 16(7), 1003–1015, doi:10.1177/0959683606hl990rp, 2006.

1000 Lillios, K. T., Blanco-González, A., Drake, B. L. and López-Sáez, J. A.: Mid-late Holocene
1001 climate, demography, and cultural dynamics in Iberia: A multi-proxy approach, Quat. Sci.
1002 Rev., 135, 138–153, doi:https://doi.org/10.1016/j.quascirev.2016.01.011, 2016.

1003 López-Sáez, J. A., Abel-Schaad, D., Pérez-Díaz, S., Blanco-González, A., Alba-Sánchez, F.,
1004 Dorado, M., Ruiz-Zapata, B., Gil-García, M. J., Gómez-González, C. and Franco-Múgica, F.:
1005 Vegetation history, climate and human impact in the Spanish Central System over the last
1006 9000 years, Quat. Int., 353, 98–122, doi:https://doi.org/10.1016/j.quaint.2013.06.034, 2014.

1007 Lukianova, R. and Alekseev, G.: Long-Term Correlation Between the Nao and Solar
1008 Activity, Sol. Phys., 224(1), 445–454, doi:10.1007/s11207-005-4974-x, 2004.

1009 Magny, M.: Holocene climate variability as reflected by mid-European lake-level
1010 fluctuations and its probable impact on prehistoric human settlements, Quat. Int., 113(1), 65–
1011 79, doi:https://doi.org/10.1016/S1040-6182(03)00080-6, 2004.

1012 Magny, M., Peyron, O., Sadori, L., Ortu, E., Zanchetta, G., Vannière, B. and Tinner, W.:
1013 Contrasting patterns of precipitation seasonality during the Holocene in the south- and north-
1014 central Mediterranean, J. Quat. Sci., 27(3), 290–296, doi:10.1002/jqs.1543, 2012.

1015 Magri, D.: Late Quaternary vegetation history at Lagaccione near Lago di Bolsena (central
1016 Italy), Rev. Palaeobot. Palynol., 106(3–4), 171–208, doi:https://doi.org/10.1016/S0034-
1017 6667(99)00006-8, 1999.

1018 Marchal, O., Cacho, I., Stocker, T. F., Grimalt, J. O., Calvo, E., Martrat, B., Shackleton, N.,
1019 Vautravers, M., Cortijo, E., Van Kreveld, S., Andersson, C., Koç, N., Chapman, M., Sbaffi,

1020 L., Duplessy, J.-C., Sarnthein, M., Turon, J.-L., Duprat, J. and Jansen, E.: Apparent long-term
1021 cooling of the sea surface in the northeast Atlantic and Mediterranean during the Holocene,
1022 Quat. Sci. Rev., 21(4–6), 455–483, doi:10.1016/S0277-3791(01)00105-6, 2002.

1023 Martín-Puertas, C., Valero-Garcés, B. L., Mata, M. P., González-Sampériz, P., Bao, R.,
1024 Moreno, A. and Stefanova, V.: Arid and humid phases in southern Spain during the last 4000
1025 years: the Zoñar Lake record, Córdoba, The Holocene, 18(6), 907–921,
1026 doi:10.1177/0959683608093533, 2008.

1027 Martín-Puertas, C., Valero-Garcés, B. L., Brauer, A., Mata, M. P., Delgado-Huertas, A. and
1028 Dulski, P.: The Iberian-Roman Humid Period (2600-1600 cal yr BP) in the Zoñar Lake varve
1029 record (Andalucía, southern Spain), Quat. Res., 71(2), 108–120,
1030 doi:10.1016/j.yqres.2008.10.004, 2009.

1031 Martín-Puertas, C., Valero-Garcés, B. L., Mata, M. P., Moreno, A., Giralt, S., Martínez-Ruiz,
1032 F. and Jiménez-Espejo, F.: Geochemical processes in a Mediterranean Lake: A high-
1033 resolution study of the last 4,000 years in Zoñar Lake, southern Spain, J. Paleolimnol., 46(3),
1034 405–421, doi:10.1007/s10933-009-9373-0, 2011.

1035 Mayewski, P. A., Rohling, E. E., Stager, J. C., Karlén, W., Maasch, K. A., Meeker, L. D.,
1036 Meyerson, E. A., Gasse, F., Kreveld, S. van, Holmgren, K., Lee-Thorp, J., Rosqvist, G.,
1037 Rack, F., Staubwasser, M., Schneider, R. R. and Steig, E. J.: Holocene climate variability,
1038 Quat. Res., 62(3), 243–255, doi:https://doi.org/10.1016/j.yqres.2004.07.001, 2004.

1039 Mercuri, A. M., Accorsi, C. A., Mazzanti, M. B., Bosi, G., Cardarelli, A., Labate, D.,
1040 Marchesini, M. and Grandi, G. T.: Economy and environment of Bronze Age settlements –
1041 Terramaras – on the Po Plain (Northern Italy): first results from the archaeobotanical research
1042 at the Terramara di Montale, Veg. Hist. Archaeobotany, 16(1), 43, doi:10.1007/s00334-006-
1043 0034-1, 2006.

1044 Morellón, M., Valero-Garcés, B., Vegas-Vilarrúbia, T., González-Sampériz, P., Romero, Ó.,
1045 Delgado-Huertas, A., Mata, P., Moreno, A., Rico, M. and Corella, J. P.: Lateglacial and
1046 Holocene palaeohydrology in the western Mediterranean region: The Lake Estanya record
1047 (NE Spain), Quat. Sci. Rev., 28(25–26), 2582–2599,
1048 doi:https://doi.org/10.1016/j.quascirev.2009.05.014, 2009.

1049 Morellón, M., Valero-Garcés, B., González-Sampériz, P., Vegas-Vilarrúbia, T., Rubio, E.,
1050 Rieradevall, M., Delgado-Huertas, A., Mata, P., Romero, Ó., Engstrom, D. R., López-
1051 Vicente, M., Navas, A. and Soto, J.: Climate changes and human activities recorded in the
1052 sediments of Lake Estanya (NE Spain) during the Medieval Warm Period and Little Ice Age,
1053 J. Paleolimnol., 46(3), 423–452, doi:10.1007/s10933-009-9346-3, 2011.

1054 Morellón, M., Anselmetti, F. S., Ariztegui, D., Brushulli, B., Sinopoli, G., Wagner, B.,
1055 Sadori, L., Gilli, A. and Pambuku, A.: Human–climate interactions in the central
1056 Mediterranean region during the last millennia: The laminated record of Lake Butrint
1057 (Albania), Spec. Issue Mediterr. Holocene Clim. Environ. Hum. Soc., 136(Supplement C),
1058 134–152, doi:10.1016/j.quascirev.2015.10.043, 2016.

1059 Moreno, A., Cacho, I., Canals, M., Grimalt, J. O., Sánchez-Goñi, M. F., Shackleton, N. and
1060 Sierro, F. J.: Links between marine and atmospheric processes oscillating on a millennial
1061 time-scale. A multi-proxy study of the last 50,000 yr from the Alboran Sea (Western

1062   Mediterranean Sea), Quat. Sci. Rev., 24(14–15), 1623–1636,
1063   doi:https://doi.org/10.1016/j.quascirev.2004.06.018, 2005.

1064   Moreno, A., Pérez, A., Frigola, J., Nieto-Moreno, V., Rodrigo-Gámiz, M., Martrat, B.,
1065   González-Sampériz, P., Morellón, M., Martín-Puertas, C., Corella, J. P., Belmonte, Á.,
1066   Sancho, C., Cacho, I., Herrera, G., Canals, M., Grimalt, J. O., Jiménez-Espejo, F., Martínez-
1067   Ruiz, F., Vegas-Vilarrúbia, T. and Valero-Garcés, B. L.: The Medieval Climate Anomaly in
1068   the Iberian Peninsula reconstructed from marine and lake records, Quat. Sci. Rev., 43, 16–32,
1069   doi:https://doi.org/10.1016/j.quascirev.2012.04.007, 2012.

1070   Nestares, T. and Torres, T. de: Un nuevo sondeo de investigación paleoambiental del
1071   Pleistoceno y Holoceno en la turbera del Padul (Granada, Andalucía). Geogaceta 23, 99-102.,
1072   1997.

1073   Oliva, M., Schulte, L. and Ortiz, A. G.: Morphometry and Late Holocene activity of
1074   solifluction landforms in the Sierra Nevada, Southern Spain, Permafr. Periglac. Process.,
1075   20(4), 369–382, 2009.

1076   Olsen, J., Anderson, N. J. and Knudsen, M. F.: Variability of the North Atlantic Oscillation
1077   over the past 5,200 years, Nat. Geosci, 5(11), 808–812, doi:10.1038/ngeo1589, 2012.

1078   Ortiz, J. E., Torres, T., Delgado, A., Julià, R., Lucini, M., Llamas, F. J., Reyes, E., Soler, V.
1079   and Valle, M.: The palaeoenvironmental and palaeohydrological evolution of Padul Peat Bog
1080   (Granada, Spain) over one million years, from elemental, isotopic and molecular organic
1081   geochemical proxies, Org. Geochem., 35(11–12), 1243–1260,
1082   doi:https://doi.org/10.1016/j.orggeochem.2004.05.013, 2004.

1083   Paillard, D., Labeyrie, L. and Yiou, P.: Macintosh Program performs time-series analysis,
1084   Eos Trans. Am. Geophys. Union, 77(39), 379–379, doi:10.1029/96EO00259, 1996.

1085   Pérez Raya, F. and López Nieto, J.: Vegetación acuática y helofítica de la depresión de Padul
1086   (Granada), Acta Bot Malacit., 16(2), 373–389, 1991.

1087   Pons, A. and Reille, M.: The holocene- and upper pleistocene pollen record from Padul
1088   (Granada, Spain): A new study, Palaeogeogr. Palaeoclimatol. Palaeoecol., 66(3), 243–263,
1089   doi:http://dx.doi.org/10.1016/0031-0182(88)90202-7, 1988.

1090   Ramos-Román, M. J., Jiménez-Moreno, G., Anderson, R. S., García-Alix, A., Toney, J. L.,
1091   Jiménez-Espejo, F. J. and Carrión, J. S.: Centennial-scale vegetation and North Atlantic
1092   Oscillation changes during the Late Holocene in the southern Iberia, Quat. Sci. Rev., 143,
1093   84–95, doi:https://doi.org/10.1016/j.quascirev.2016.05.007, 2016.

1094   Reimer, P. J., Bard, E., Bayliss, A., Beck, J. W., Blackwell, P. G., Ramsey, C. B., Buck, C.
1095   E., Cheng, H., Edwards, R. L., Friedrich, M., Grootes, P. M., Guilderson, T. P., Haflidason,
1096   H., Hajdas, I., Hatté, C., Heaton, T. J., Hoffmann, D. L., Hogg, A. G., Hughen, K. A., Kaiser,
1097   K. F., Kromer, B., Manning, S. W., Niu, M., Reimer, R. W., Richards, D. A., Scott, E. M.,
1098   Southon, J. R., Staff, R. A., Turney, C. S. M. and van der Plicht, J.: IntCal13 and Marine13
1099   Radiocarbon Age Calibration Curves 0–50,000 Years cal BP, Radiocarbon, 55(4), 1869–
1100   1887, doi:10.2458/azu_js_rc.55.16947, 2013.

1101 Riera, S., Wansard, G. and Julià, R.: 2000-year environmental history of a karstic lake in the
1102 Mediterranean Pre-Pyrenees: the Estanya lakes (Spain), {CATENA}, 55(3), 293–324,
1103 doi:https://doi.org/10.1016/S0341-8162(03)00107-3, 2004.

1104 Riera, S., López-Sáez, J. A. and Julià, R.: Lake responses to historical land use changes in
1105 northern Spain: The contribution of non-pollen palynomorphs in a multiproxy study, Rev.
1106 Palaeobot. Palynol., 141(1–2), 127–137, doi:https://doi.org/10.1016/j.revpalbo.2006.03.014,
1107 2006.

1108 Roberts, N., Brayshaw, D., Kuzucuoğlu, C., Perez, R. and Sadori, L.: The mid-Holocene
1109 climatic transition in the Mediterranean: Causes and consequences, The Holocene, 21(1), 3–
1110 13, doi:10.1177/0959683610388058, 2011.

1111 Rodrigo-Gámiz, M., Martínez-Ruiz, F., Rodríguez-Tovar, F. J., Jiménez-Espejo, F. J. and
1112 Pardo-Igúzquiza, E.: Millennial- to centennial-scale climate periodicities and forcing
1113 mechanisms in the westernmost Mediterranean for the past 20,000 yr, Quat. Res., 81(1), 78–
1114 93, doi:https://doi.org/10.1016/j.yqres.2013.10.009, 2014.

1115 Sadori, L., Jahns, S. and Peyron, O.: Mid-Holocene vegetation history of the central
1116 Mediterranean, The Holocene, 21(1), 117–129, doi:10.1177/0959683610377530, 2011.

1117 Sadori, L., Giraudi, C., Masi, A., Magny, M., Ortu, E., Zanchetta, G. and Izdebski, A.:
1118 Climate, environment and society in southern Italy during the last 2000 years. A review of
1119 the environmental, historical and archaeological evidence, Spec. Issue Mediterr. Holocene
1120 Clim. Environ. Hum. Soc., 136(Supplement C), 173–188,
1121 doi:10.1016/j.quascirev.2015.09.020, 2016.

1122 Sanz de Galdeano, C., El Hamdouni, R. and Chacón, J.: Neotectónica de la fosa del Padul y
1123 del Valle de Lecrín, Itiner. Geomorfológicos Por Andal. Orient. Publicacions Univ. Barc.
1124 Barc., 65–81, 1998.

1125 Sicre, M.-A., Jalali, B., Martrat, B., Schmidt, S., Bassetti, M.-A. and Kallel, N.: Sea surface
1126 temperature variability in the North Western Mediterranean Sea (Gulf of Lion) during the
1127 Common Era, Earth Planet. Sci. Lett., 456, 124–133,
1128 doi:http://dx.doi.org/10.1016/j.epsl.2016.09.032, 2016.

1129 Sonett, C. P. and Suess, H. E.: Correlation of bristlecone pine ring widths with atmospheric
1130 14C variations: a climate-Sun relation, Nature, 307(5947), 141–143, doi:10.1038/307141a0,
1131 1984.

1132 Steinhilber, F., Beer, J. and Fröhlich, C.: Total solar irradiance during the Holocene,
1133 Geophys. Res. Lett., 36(19), n/a–n/a, doi:10.1029/2009GL040142, 2009.

1134 Trouet, V., Esper, J., Graham, N. E., Baker, A., Scourse, J. D. and Frank, D. C.: Persistent
1135 Positive North Atlantic Oscillation Mode Dominated the Medieval Climate Anomaly,
1136 Science, 324(5923), 78, doi:10.1126/science.1166349, 2009.

1137 Valle, F.: Mapa de series de vegetación de Andalucía 1: 400 000, Editorial Rueda., 2003.

1138 Valle Tendero, F.: Modelos de Restauración Forestal: Datos botánicos aplicados a la gestión
1139 del Medio Natural Andaluz II: Series de vegetación, Cons. Medio Ambiente Junta Andal.
1140 Sevilla, 2004.

1141 Villegas Molina, F.: Laguna de Padul: Evolución geológico-histórica, Estud. Geográficos,
1142 28(109), 561, 1967.

1143 Zanchettin, D., Rubino, A., Traverso, P. and Tomasino, M.: Impact of variations in solar
1144 activity on hydrological decadal patterns in northern Italy, J. Geophys. Res. Atmospheres,
1145 113(D12), n/a–n/a, doi:10.1029/2007JD009157, 2008.

1146
Figures and tables
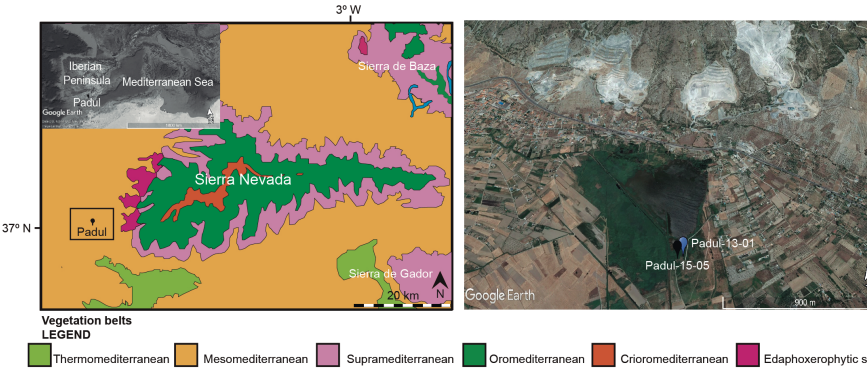
1148

1149 **Figure 1.** Location of Padul in Sierra Nevada, southern Iberian Peninsula. Panel on the left is
1150 the map of the vegetation belts in the Sierra Nevada (Modified from REDIAM. Map of the
1151 vegetation series of Andalucía:
1152 http://laboratoriorediam.cica.es/VisorGenerico/?tipo=WMS&url=http://www.juntadeandaluci
1153 a.es/medioambiente/mapwms/REDIAM_Series_Vegetacion_Andalucia?). The inset map is
1154 the Google earth image of the Iberian Peninsula in the Mediterranean region. Panel on the
1155 right is the Google earth image (http://www.google.com/earth/index.html) of Padul peat bog
1156 area showing the coring locations.

1158
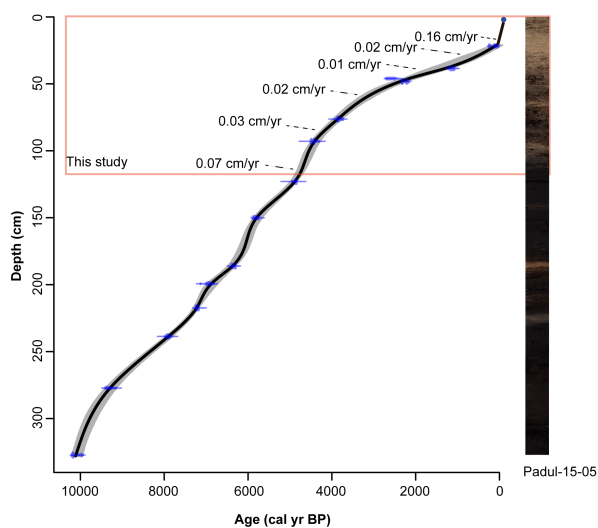
Figure 2. Photo of the Padul-15-05 sediment core with the age-depth model showing the part
of the record that was studied here (red rectangle). The sediment accumulation rates (SAR)
between individual segments are marked. See the body of the text for the explanation of the
age reconstructions.

1163
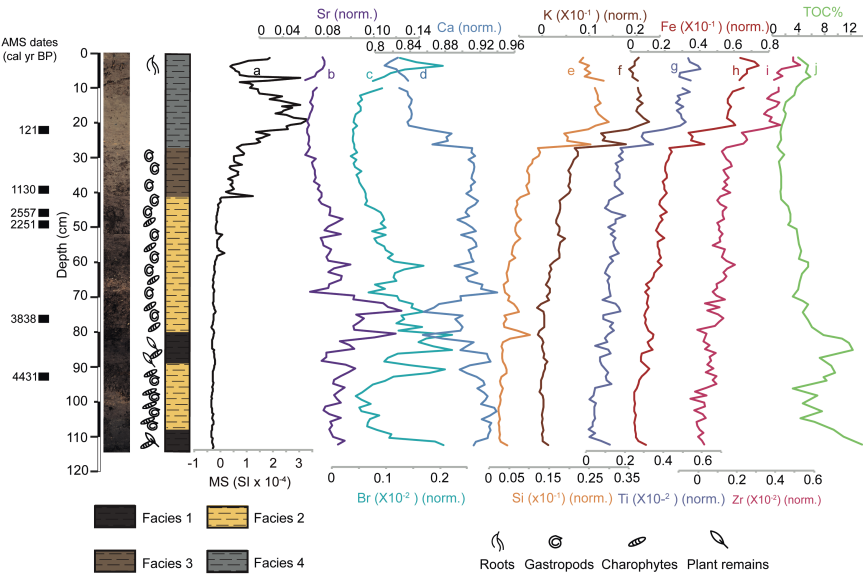
Figure 3. Lithology, facies interpretation with paleontology, magnetic susceptibility (MS), and geochemical (X-ray fluorescence (XRF) and total organic carbon (TOC) data from the Padul-15-05 record. XRF elements are represented normalized by the total counts. (a) Magnetic susceptibility (MS; SI units). (b) Strontium normalized (Sr; norm.). (c) Bromine norm. (Br; norm.). (d) Calcium normalized. (Ca; norm.). (e) Silica normalized (Si; norm.). (f) Potassium normalized (K; norm.). (g) Titanium normalized (Ti; norm.). (h) Iron normalized (Fe; norm.). (i) Zirconium normalized (Zr; norm.). (j) Total organic carbon (TOC %). AMS radiocarbon dates (cal yr BP) are shown on the left.

1166
1167
1168
1169
1170
1171
1172
1173

1174
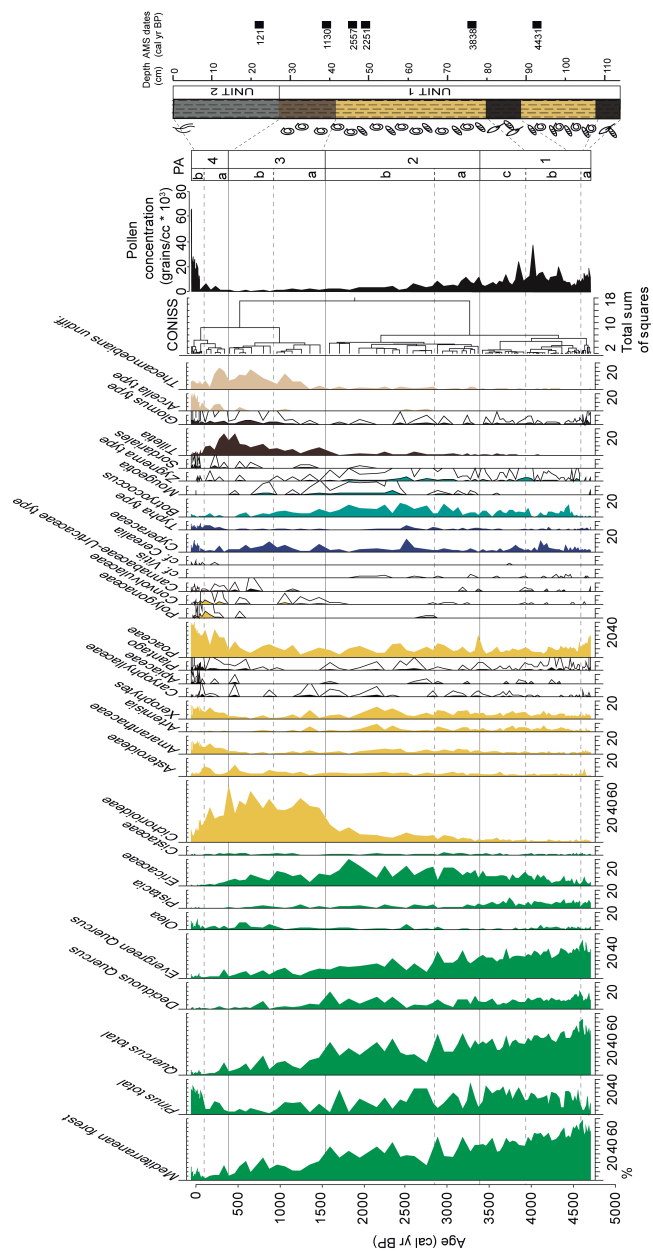
1175

1176

Figure 4. Percentages of selected pollen taxa and non-pollen palynomorphs (NPPs) from the Padul-15-05 record, calculated with respect to terrestrial pollen sum. Silhouettes show 7-time exaggerations of pollen percentages. Pollen zonation, pollen concentration (grains/cc), lithology and AMS radiocarbon dates are shown on the right. Tree and shrubs are showing in green, herbs and grasses in yellow, aquatics in dark blue, algae in blue, fungi in brown and thecamoebians in beige. The Mediterranean forest taxa category is composed of *Quercus* total, *Olea, Phillyrea* and *Pistacia*. The xerophyte group includes *Artemisia, Ephedra*, and Amaranthaceae. PA = Pollen zones.

1187
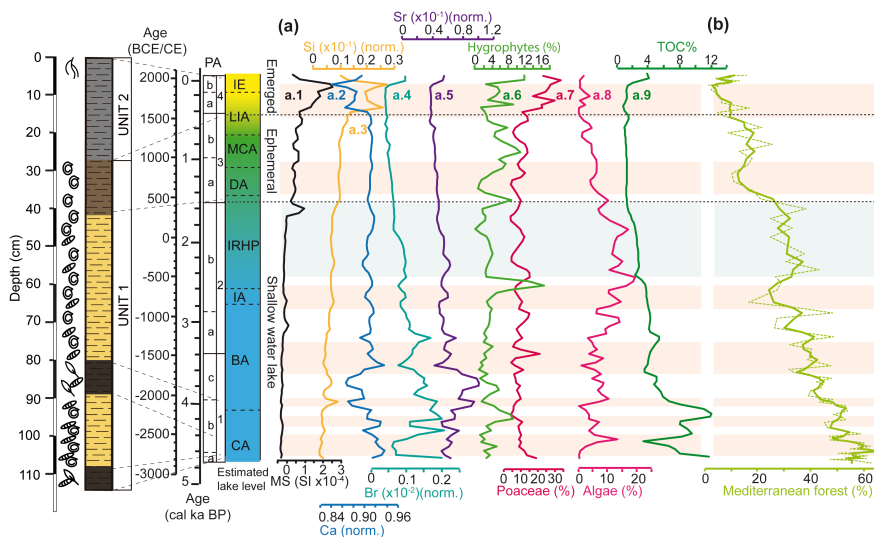
Figure 5. Estimated lake level evolution and regional palynological component from the last ca. 4700 yr based on the synthesis of determinate proxies from the Padul-15-05 record: (a) Proxies used to estimate the water table evolution from the Padul-15-05 record (proxies were resampled at 50 yr (lineal interpolation) using Past software http://palaeo-electronica.org/2001_1/past/issue1_01.htm). [(a.1) Magnetic Susceptibility (MS) in SI; (a.2) Silica normalized (Si; norm.); (a.3) Calcium normalized (Ca; norm.); (a.4) Bromine normalized (Br; norm.); (a.5) Strontium normalized (Sr; norm.); (a.6) Hygrophytes (%); (a.7) Poaceae (%); (a.8) Algae (%) (a.9) Total organic carbon (TOC %)] (b) Mediterranean forest taxa, with a smoothing of three-point in bold. Pink and blue shading indicates Holocene arid and humid regionally events, respectively. See the body of the text for the explanation of the lake level reconstruction. Mediterranean forest smoothing was made using Analyseries software (Paillard et al., 1996). PA = Pollen Zones; CA = Copper Age; BA = Bronze Age; IA = Iron Age; IRHP = Iberian Roman Humid Period; DA = Dark Ages; MCA = Medieval Climate Anomaly; LIA = Little Ice Age; IE = Industrial Era.

1202

1203
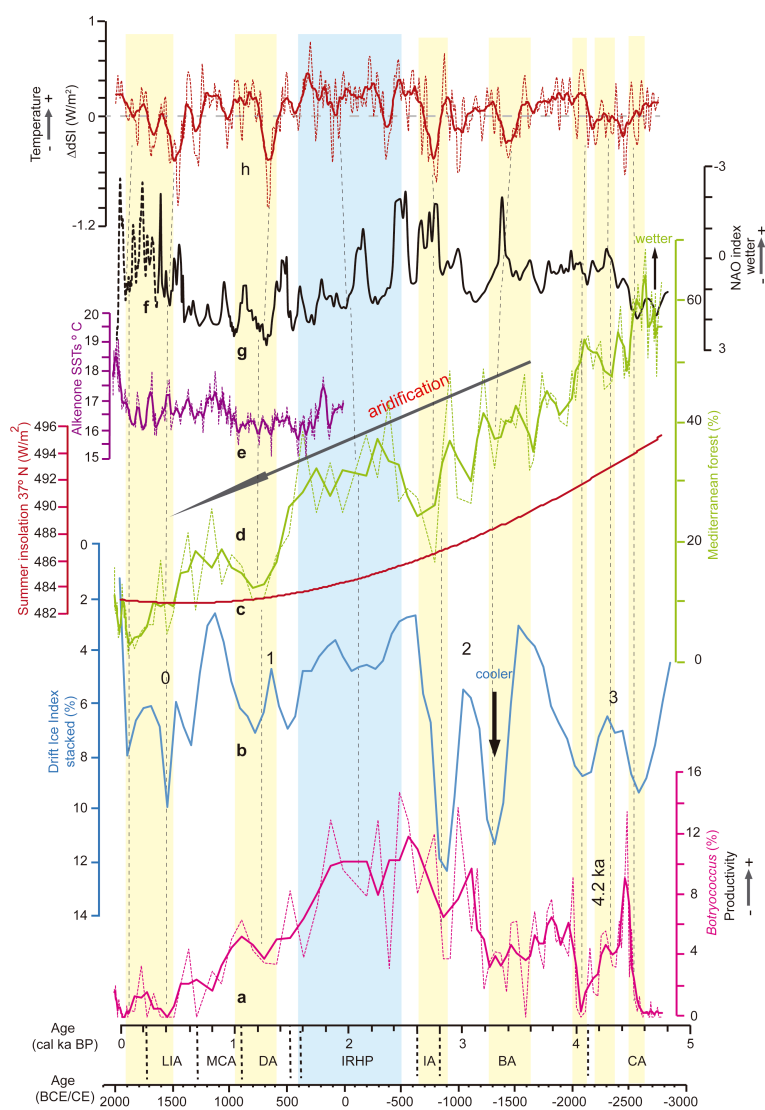
Figure 6. Comparison of the last ca. 4700 yr between different pollen taxa from the Padul-15-05 record, summer insolation for the Sierra Nevada latitude, eastern Mediterranean humidity and North Atlantic temperature. (a) *Botryococcus* from the Padul-15-05 record, with a smoothing of three-point in bold (this study). (b) Drift Ice Index (reversed) from the North Atlantic (Bond et al., 2001). (c) Summer insolation calculated for 37º N (Laskar et al., 2004). (d) Mediterranean forest taxa from the Padul-15-05 record, with a smoothing of three-

point in bold (this study). (e) Alkenone-SSTs from the Gulf of Lion (Sicre et al., 2016), with a smoothing of four-point in bold. (f) North Atlantic Oscillation (NAO) index from a climate proxy reconstruction from Morocco and Scotland (Trouet et al., 2009). (g) North Atlantic Oscillation (NAO) index (reversed) from a climate proxy reconstruction from Greenland (Olsen et al., 2012). (h) Total solar irradiance reconstruction from cosmogenic radionuclide from a Greenland ice core (Steinhilber et al., 2009), with a smoothing of twenty-one-point in bold. Note that the magnitude of the different curves is not in the same scale. Yellow and blue shading correspond with arid (and cold) and humid (and warm) periods, respectively. Grey dash lines show a tentative correlation between arid and cold conditions and the decrease in the Mediterranean forest and *Botryococcus*. Mediterranean forest, *Botryococcus* and solar irradiance smoothing was made using Analyseries software (Paillard et al., 1996), Alkenone-SSTs smoothing was made using Past software (http://palaeo-electronica.org/2001_1/past/issue1_01.htm). A linear r (Pearson) correlation was calculated between *Botryococcus* (detrended) and Drift Ice Index (Bond et al., 2001; $r = -0.63$; $p < 0.0001$; between ca. 4700 to 1500 cal ka BP – r=-0.48; $p < 0.0001$ between 4700 and -65 cal yr BP). Previously, the data were detrended (only in *Botryococcus*), resampled at 70-yr (linear interpolation) in order to obtain equally spaced time series and smoothed to three-point average. CA = Copper Age; BA = Bronze Age; IA = Iron Age; IRHP = Iberian Roman Humid Period; DA = Dark Ages; MCA = Medieval Climate Anomaly; LIA = Little Ice Age; IE = Industrial Era.
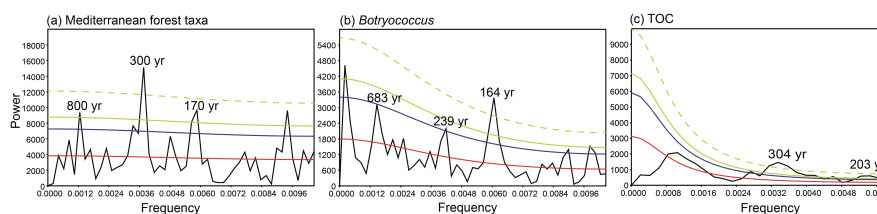
Figure 7. Spectral analysis of (a) Mediterranean forest taxa and (b) *Botryococcus* (mean sampling space = 47 yr) and (c) TOC (mean sampling space = 78 yr) from the Padul-15-05. The significant periodicities above confident level are shown. Confidence level 90 % (blue line), 95 % (green line), 99 % (green dash line) and AR (1) red noise (red line). Spectral analysis was made with Past software (http://palaeo-electronica.org/2001_1/past/issue1_01.htm).

1240

1241

1242
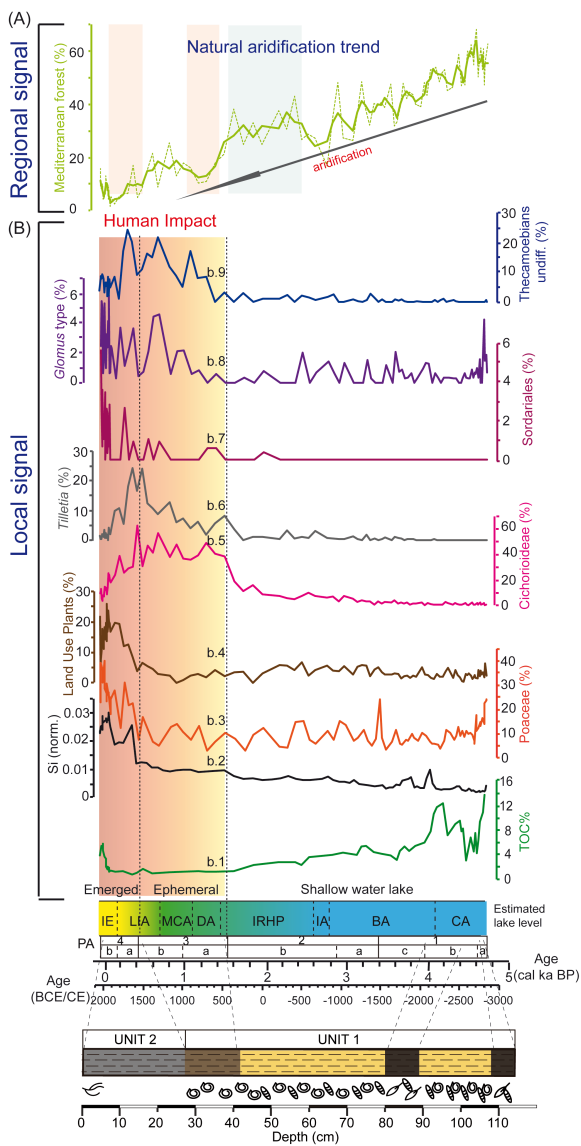
Figure 8. Comparison of the last ca. 4700 yr between regional climatic proxies and local human activity indicators from the Padul-15-05 record. (a) Mediterranean forest taxa, with a

1245   smoothing of three-point in bold. (b) Local human activities indicators [(b.1) Total organic
1246   carbon (TOC %), soil erosion indicator; (b.2) Si normalized (Si, norm.), soil erosion
1247   indicator; (b.3) Poaceae (%), lake drained and/or cultivars indicator; (b.4) Land Use Plants
1248   (%), cultivar indicator; (b.5) Cichorioideae (%), livestock occurrence indicator; (b.6) *Tilletia*
1249   (%), farming indicator; (b.7) Sordariales (%), livestock indicator; (b.8) Glomus type, soil
1250   erosion, (b. 9) Thecamoebians undiff. (%), livestock indicator]. Degraded yellow to red
1251   shading correspond with the time when we have evidence of human shaping the environment
1252   since ca. 1550 cal yr BP to Present. Previously to that period there is a lack of clear evidences
1253   of human impact in the area. Land use plants is composed by Polygonaceae, Amaranthaceae,
1254   Convolvulaceae, *Plantago*, Apiaceae and Cannabaceae-Urticaceae type.

1255 **Table 1.** Age data for Padul-15-05 record. All ages were calibrated using R-code package
1256 'clam 2.2' employing the calibration curve IntelCal 13 (Reimer et al., 2013) at 95 % of
1257 confident range.

1258 *Sample number assigned at radiocarbon laboratory

Laboratory number	Core	Material	Depth (cm)	Age (^{14}C yr BP ± 1σ)	Calibrated age (cal yr BP) 95 % confidence interval	Median age (cal yr BP)
Reference ages			0	2015CE	-65	-65
D-AMS 008531	Padul-13-01	Plant remains	21.67	103 ± 24	23-264	127
Poz-77568	Padul-15-05	Org. bulk sed.	38.46	1205 ± 30	1014-1239	1130
BETA-437233	Padul-15-05	Plant remains	46.04	2480 ± 30	2385-2722	2577
Poz-77569	Padul-15-05	Org. bulk sed.	48.21	2255 ± 30	2158-2344	2251
BETA-415830	Padul-15-05	Shell	71.36	3910 ± 30	4248-4421	4343
BETA-437234	Padul-15-05	Plant remains	76.34	3550 ± 30	3722-3956	3838
BETA-415831	Padul-15-05	Org. bulk sed.	92.94	3960 ± 30	4297-4519	4431
Poz-74344	Padul-15-05	Plant remains	122.96	4295 ± 35	4827-4959	4871
BETA-415832	Padul-15-05	Plant remains	150.04	5050 ± 30	5728-5900	5814
Poz-77571	Padul-15-05	Plant remains	186.08	5530 ± 40	6281-6402	6341
Poz-74345	Padul-15-05	Plant remains	199.33	6080 ± 40	6797-7154	6935
BETA-415833	Padul-15-05	Org. bulk sed.	217.36	6270 ± 30	7162-7262	7212
Poz-77572	Padul-15-05	Org. bulk sed.	238.68	7080 ± 50	7797-7999	7910
Poz-74347	Padul-15-05	Plant remains	277.24	8290 ± 40	9138-9426	9293
BETA-415834	Padul-15-05	Plant remains	327.29	8960 ± 30	9932-10221	10107

1259

1260

1261 **Table 2.** Linear r (Pearson) correlation between geochemical elements from the Padul-15-05
1262 record. Statistical treatment was performed using the Past software (http://palaeo-
1263 electronica.org/2001_1/past/issue1_01.htm).

1264

	Si	K	Ca	Ti	Fe	Zr	Br	Sr
Si		8.30E-80	2.87E-34	7.47E-60	3.22E-60	5.29E-44	0.001152	7.79E-09
K	0.98612		7.07E-29	6.05E-60	8.20E-68	1.77E-51	0.00030317	5.38E-12
Ca	-0.88096	-0.84453		6.09E-42	5.81E-39	8.10E-34	0.35819	0.26613
Ti	0.96486	0.96501	-0.91794		1.74E-74	1.12E-57	0.074223	8.88E-07
Fe	0.96546	0.97577	-0.90527	0.98224		2.77E-66	0.051072	3.32E-08
Zr	0.92566	0.94789	-0.8783	0.96109	0.97398		0.054274	7.16E-08
Br	-0.31739	-0.3506	-0.091917	-0.17755	-0.19372	-0.19116		4.03E-18
Sr	-0.53347	-0.61629	0.11113	-0.46426	-0.51386	-0.50295	0.72852	

1265

1266

1267

1268

1269

1270

1271

1272

1273

1274

1275

1276

1277

1278

1279

1280

Study site

   2.1 Regional setting: Sierra Nevada climate and vegetation

[1]

The Padul basin is situated in the mesomediterranean vegetation belt at approximately 725 m elevation in the southeastern part of the Granada Basin.